Stem Cell Reports
Article

OPEN ACCESS

RHOA GTPase Controls YAP-Mediated EREG Signaling in Small Intestinal Stem Cell Maintenance

Ming Liu,[1,2,4] Zheng Zhang,[1,4] Leesa Sampson,[1] Xuan Zhou,[1] Kodandaramireddy Nalapareddy,[1] Yuxin Feng,[1] Shailaja Akunuru,[1] Jaime Melendez,[1,3] Ashley Kuenzi Davis,[1] Feng Bi,[2] Hartmut Geiger,[1] Mei Xin,[1] and Yi Zheng[1,*]

[1]Division of Experimental Hematology & Cancer Biology, Cincinnati Children's Hospital Research Foundation, 3333 Burnet Avenue, Cincinnati, OH 45229, USA
[2]Department of Medical Oncology, West China Hospital, Sichuan University, Chengdu, Sichuan Province 610041, China
[3]Laboratorio de Bioquímica y Biología Molecular Depto. Farmacia Facultad de Química, P. Universidad Católica de Chile, Santiago, Chile
[4]Co-first author
*Correspondence: yi.zheng@cchmc.org
https://doi.org/10.1016/j.stemcr.2017.10.004

SUMMARY

RHOA, a founding member of the Rho GTPase family, is critical for actomyosin dynamics, polarity, and morphogenesis in response to developmental cues, mechanical stress, and inflammation. In murine small intestinal epithelium, inducible RHOA deletion causes a loss of epithelial polarity, with disrupted villi and crypt organization. In the intestinal crypts, RHOA deficiency results in reduced cell proliferation, increased apoptosis, and a loss of intestinal stem cells (ISCs) that mimic effects of radiation damage. Mechanistically, RHOA loss reduces YAP signaling of the Hippo pathway and affects YAP effector epiregulin (EREG) expression in the crypts. Expression of an active *YAP* (S112A) mutant rescues ISC marker expression, ISC regeneration, and ISC-associated Wnt signaling, but not defective epithelial polarity, in *RhoA* knockout mice, implicating YAP in RHOA-regulated ISC function. EREG treatment or active β-catenin $Catnb^{lox(ex3)}$ mutant expression rescues the *RhoA* KO ISC phenotypes. Thus, RHOA controls YAP-EREG signaling to regulate intestinal homeostasis and ISC regeneration.

INTRODUCTION

Intestinal epithelium, one of the most vigorously self-renewing tissues in an adult mammal, is composed of four major cell types: absorptive enterocytes, mucus-secreting goblet cells, antimicrobial Paneth cells, and hormone-secreting enteroendocrine cells (Barker and Clevers, 2010; Barker et al., 2007). More differentiated cell types reside within the villus, while the base of each villus is surrounded by multiple epithelial crypt invaginations (Clevers, 2013). At the bottom of each crypt, crypt base columnar cells (CBCs) (Cheng and Leblond, 1974) occupy cell positions +1 through +5 from the base and are intercalated between Paneth cells, which together constitutes a stem cell niche (Sato et al., 2011; Snippert et al., 2010).

The CBCs, containing intestinal stem cell (ISC) activity, proliferate constantly and give rise to rapidly proliferating transient amplifying cells just above Paneth cells. Transient amplifying cells then migrate upward and differentiate at the crypt-villus boundary into one of the four mature cell types (Tian et al., 2015). Several molecular markers have been used to identify ISCs, including *Lgr5*, *Ascl2*, *Olfm4*, and *Bmi1* (Barker and Clevers, 2010; Barker et al., 2007; van der Flier et al., 2009). The Lgr5-positive cells are actively cycling, long lived, and give rise to all four epithelial lineages (Sato et al., 2011; Snippert et al., 2010). Single Lgr5-expressing ISCs can be cultured *in vitro* to form long-lived, self-organizing crypt-villus organoids in the absence of non-epithelial niche cells (Sato and Clevers, 2013; Sato et al., 2009, 2011).

The regeneration and differentiation process of the small intestine is stringently regulated to ensure a balanced homeostasis. Primarily known as an important regulator in organ size control and cell proliferation (Zhao et al., 2010), the Hippo/Yes-Associated Protein (YAP) pathway has emerged recently as an important regulator of ISC regeneration and intestinal tumorigenesis (Barry and Camargo, 2013; Hong et al., 2016). YAP1 and TAZ have been shown to promote ISC proliferation (Imajo et al., 2015), but surprisingly, mice with depleted YAP1 and/or TAZ protein in the intestine have normal homeostasis (Azzolin et al., 2014; Barry et al., 2013; Cai et al., 2015), suggesting that YAP1 and TAZ are dispensable under normal conditions. Further studies show that YAP1 is involved in intestinal regeneration after drug- or irradiation-induced injury (Gregorieff et al., 2015; Taniguchi et al., 2015), and the YAP1 target, epidermal growth factor receptor ligand EREG, modulates ISC proliferation and regeneration (Gregorieff et al., 2015). Multiple studies suggest that the Hippo-YAP pathway interacts with the Wnt/β-catenin pathway (Pinto et al., 2003; van der Flier and Clevers, 2009) to regulate the function of ISCs (Azzolin et al., 2014; Barry and Camargo, 2013; Cai et al., 2015; Imajo et al., 2012). However, conflicting interpretations of these studies led to the proposal that YAP may both enhance and inhibit Wnt signaling in ISCs (Azzolin et al., 2014; Barry and Camargo, 2013; Imajo et al., 2012; Rosenbluh

et al., 2012), possibly reflecting the complexity of the signaling network in ISC regulation.

While many of the current studies focus on the intracellular signaling mechanisms of ISCs, the apical-basal polarity and cell adhesion junctions play key roles in intestinal epithelium morphogenesis. As a key member of the Rho guanosine triphosphatase (GTPase) family, RHOA has been found to be involved in regulating tissue-specific cytoskeleton dynamics, cell adhesion, survival, cell-cycle progression, and transcription (Etienne-Manneville and Hall, 2002; Wang and Zheng, 2007). RHOA acts as a molecular switch to control signal transduction by shifting between a guanosine diphosphate (GDP)-bound, inactive form and a GTP-bound, active form (Etienne-Manneville and Hall, 2002; Karlsson et al., 2009; Liu et al., 2012; Wang and Zheng, 2007). Dysfunction of RHOA and related GTPases can cause cancer, neurological abnormalities, immunological disorders, and several other diseases (Wang and Zheng, 2007; Zhou and Zheng, 2013). Interestingly, in the Hippo pathway, YAP1 and TAZ transcriptional activities are regulated by mechanical actomyosin signal and G-protein-coupled receptor (GPCR)-mediated extracellular signals through Rho GTPases (Dupont et al., 2011; Rauskolb et al., 2014; Yu et al., 2012; Zhao et al., 2012), suggesting a connection between RHOA and Hippo-mediated transcription.

In the current work, we use an intestinal epithelium-specific inducible gene deletion in a mouse model of Villin-CreERT2;*RhoA*$^{flox/flox}$ to define the physiological function and molecular mechanisms of RHOA in ISC regulation. Our study shows that RHOA-mediated YAP-EREG signaling plays a critical role during intestine homeostasis and ISC regeneration, implicating a relationship between RHOA-controlled epithelial integrity/polarity and intracellular YAP/Wnt signaling in ISC regulation.

RESULTS

Inducible Deletion of RhoA Causes Defects in Small Intestinal Epithelium

RHOA is unanimously expressed throughout the small intestine in adult mice, including crypt and villi (Figures S1A and S1B). Inside the crypt, RHOA protein is detected in both Lgr5^{-}GFP^{+} ISCs and Lgr5^{-}GFP^{-} Paneth cells in the small intestine of Lgr5-EGFP-IRES-CreERT2 knockin mice (Figures S1A and S1B).

To investigate the function of RHOA in mammalian intestinal epithelium, we generated an inducible intestine-specific *RhoA*-ablation mouse line, which uses the intestinal epithelium-specific *Villin* promoter to deliver tamoxifen-inducible Cre activity in the intestine. Villin-CreERT2; *RhoA*$^{fl/fl}$ mice (hereafter called *RhoA* knockout [KO]) and respective control wild-type mice *RhoA*$^{fl/fl}$ (hereafter called WT) were injected with tamoxifen intraperitoneally, twice a day for 3 straight days at 4–8 weeks of age. One day post tamoxifen administration, the *RhoA* KO mice were depleted of the *RhoA* gene and protein in the small intestine but not in the surrounding stroma (Figures S1C, S1D, and 1A). Compensatory expression of other Rho GTPase family members such as Rac1 and CDC42 was not detected, and the downstream effector of RHOA, phospho-MLC2, was downregulated upon RHOA deletion (Figure 1A). H&E staining of duodenum in *RhoA* KO mice revealed a severe disruption of crypt-villus architecture compared with WT mice (Figure 1B). The villi in the *RhoA* KO mice were relatively intact but noticeably shorter than that of WT mice (Figure 1B). Transmission electron microscopy analysis confirmed that the intestinal epithelial architecture was disorganized in *RhoA* KO mice (Figure S2A). Similar but more moderate structural defects in villi and crypts were observed in jejunum and ileum (Figures S2B and S2C). We chose duodenum as the focus of this study.

Further analysis comparing RHOA and E-cadherin protein expression in WT and KO duodenum confirms a complete deletion of RHOA in both villi and crypts of KO mice, while E-cadherin levels were reduced with a disrupted expression pattern in the KO (Figures 1C and 1D). Noticeably, there is no detectable difference between heterozygous *RhoA* KO (Villin-CreERT2^{+}; *RhoA*$^{fl/wt}$) mice and control WT (*RhoA*$^{fl/fl}$) litters (data not shown), indicating that there is no haplodeficient effect with *RhoA* gene in the small intestine.

Loss of RhoA Disrupts Epithelial Polarity, Adhesion, and Organization in the Small Intestine

RHOA is involved in actin stress fiber formation, actomyosin contractility, focal adhesion, and adherens junction (AJ) complex (Kaibuchi et al., 1999; Melendez et al., 2011; Rajasekaran et al., 2001). To further characterize the intestinal defects in *RhoA* KO mice, we analyzed the transcription pattern of markers for AJ, polarity, and basolateral compartments. The transcription expression of polarity-regulating molecules *Par3* and *Par6* was significantly reduced in *RhoA* KO intestine (Figure 2A) while the mRNA level of adhesion molecules *E-cadherin* and *β-Catenin* were not significantly altered, suggesting disrupted epithelial polarity. Immunofluorescence staining found that in *RhoA* KO mice, ion transporter Na^{+},K^{+}-ATPase, a basolateral marker, was more diffusely localized, confirming the polarity defect (Figure 2B). Analysis of actin cytoskeleton using phalloidin staining showed a disrupted junctional actin network in *RhoA* KO intestinal epithelial cells (Figure 2C), consistent with the disruption of the E-cadherin complex (Figure 1D).

We next examined whether loss of RHOA affects different cell types in small intestine. Paneth cells are

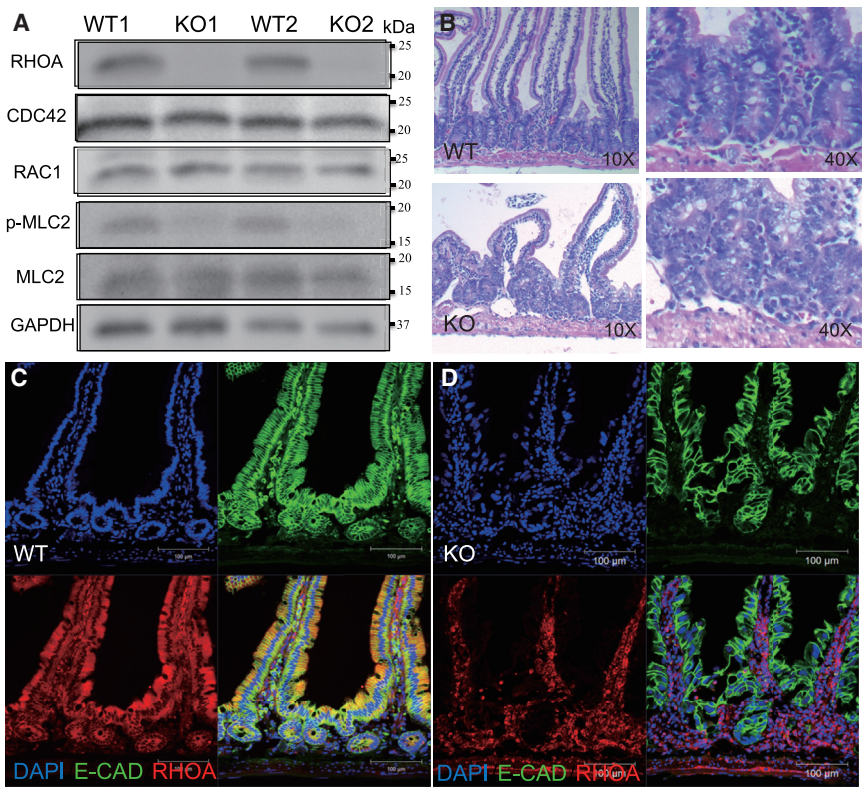

Figure 1. Conditional Deletion of RhoA in the Small Intestine Causes Defects in Epithelial Architecture

(A) Western blotting of RHOA, Cdc42, Rac1, and effectors of RHOA (MLC2 and p-MLC2) in isolated small intestinal crypts from 1- to 2-month-old control WT or *RhoA* KO mice.

(B) Representative H&E staining of control WT or *RhoA* KO duodenum sections.

(C and D) Representative immunofluorescence by anti-RHOA and anti-E-cadherin in control WT (C) or *RhoA* KO (D) duodenum sections.

exclusively located at the bottom of the crypts in WT intestine, as shown by lysozyme immunostaining; in the KO mice, most Paneth cells remained in the crypts but the villi/crypt structures were disrupted (Figures S3A and S3B). In addition, the number and localization of goblet cells and enteroendocrine cells marked by mucin-2 and chromogranin A staining, respectively, were unaffected by *RhoA* KO (Figures S3C and S3D). We conclude that RHOA is critically involved in basolateral polarity, cell adhesion, and epithelium organization in the small intestine.

Loss of RhoA Reduces Proliferation and Induces Apoptosis in Small Intestinal Crypts

RHOA has been implicated in regulating epithelial cell proliferation in the small intestine (Benoit et al., 2009), and RHOA-regulated cell adhesion/polarity is closely related to cell-cycle regulation. We next examined whether the crypt cell proliferation and cell cycle are affected by RHOA loss of function. The number of proliferating crypt cells marked by Ki67 (non-G_0 cycling cells) (Figure 2D) and phosphor-histone H3 (M-phase cells) (Figure S3E) are both dramatically decreased in *RhoA* KO intestinal tissue, which may account for the disorganized epithelial structure. Reduced proliferation occurs in all sections of the intestine, including duodenum, jejunum, and ileum (data not shown), suggesting that RHOA is critical for cell proliferation in the whole small intestine. Recent genetic studies have revealed a critical function of RHOA during mitosis in different biological contexts including blood progenitor cells, keratinocytes, and mouse embryonic fibroblasts (Jackson et al., 2011; Melendez et al., 2011; Zhou et al., 2013). Interestingly, RHOA deficiency in small intestine also induced multinucleated cells (Figure S3F), suggesting a mitotic arrest.

Aside from the effect on proliferation, the *RhoA* KO increased the cleaved caspase-3-positive cells significantly throughout the crypts and villi (Figure S3G, quantified in Figure 2E). Consistently, total cleaved caspase-3 protein level was dramatically increased in *RhoA* KO epithelium as found by western blotting (Figure 2F), which could, at least in part, account for the partial loss of the crypt upon RHOA deletion. Molecularly, RHOA deletion caused a reduced pro-survival signal marked by Bcl-2, with no obvious change of pro-apoptotic proteins such as p53 (Figure 2F), indicating an altered apoptotic mechanism.

Inducible RhoA Deletion Leads to a Loss of Intestinal Stem Cells and Reduced Canonical Wnt Signaling *In Vivo* and *In Vitro*

Disrupted crypts and reduced proliferation in *RhoA* KO small intestine is indicative of ISC malfunction. To

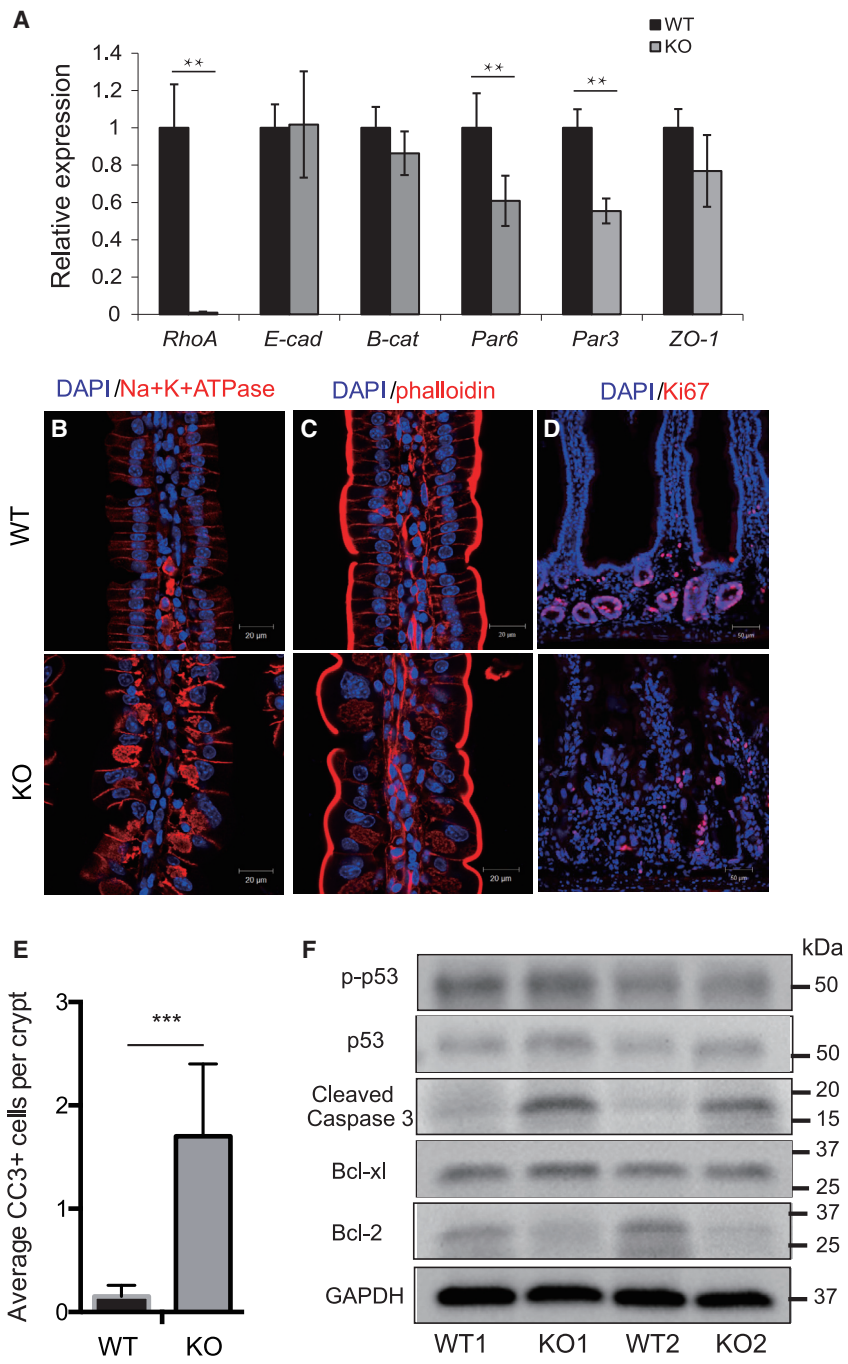

Figure 2. Loss of RhoA Disrupts Epithelial Polarity and Adhesion, while Reducing Proliferation and Inducing Apoptosis in Small Intestine

(A) qRT-PCR analysis showing gene expression of cell junction and polarity markers in control WT and *RhoA* KO small intestine. Data are normalized to GAPDH expression; n = 3 mice per genotype. Error bars represent SD from three independent experiments.

(B–D) Representative immunofluorescence staining of Na^+,K^+-ATPase α (B), phalloidin (C), and Ki67 (D) in control WT and *RhoA* KO duodenum.

(E) Quantification of cleaved caspase-3-positive cells per crypt in control WT and *RhoA* KO duodenum. n = 4 mice for each genotype. Error bars represent SD from three independent experiments.

(F) Western blotting of apoptotic related proteins Bcl-2, Bcl-xL, p53, p-P53, and cleaved caspase-3 in duodenal crypts isolated from control and *RhoA* KO mice.

**p < 0.01, ***p < 0.001.

determine the requirement of RHOA in ISCs, we crossed Lgr5-EGFP-IRES-CreERT2 mouse (Barker et al., 2007), which has the eGFP marking $Lgr5^+$ ISCs in the crypts, with *RhoA* KO and WT mice (the CreERT2 in this model could not effectively delete *RhoA* gene upon tamoxifen induction; data not shown). In this model, $Lgr5^-eGFP^+$ ISCs were drastically reduced in small intestine crypts 2 days after tamoxifen induction (Figure S4A). An *in situ* hybridization analysis showed that the ISC marker *Olfm4* was also dramatically decreased in RHOA-depleted small intestine (Figure 3A). A qRT-PCR test confirmed that three ISC markers, i.e., *Lgr5*, *Olfm4*, and *Ascl2*, were significantly reduced in *RhoA* KO crypts (Figure 3C).

Since canonical Wnt signaling is associated with and is required for self-renewal of ISCs and ISC-niche interaction (Pinto et al., 2003; van der Flier and Clevers, 2009), we

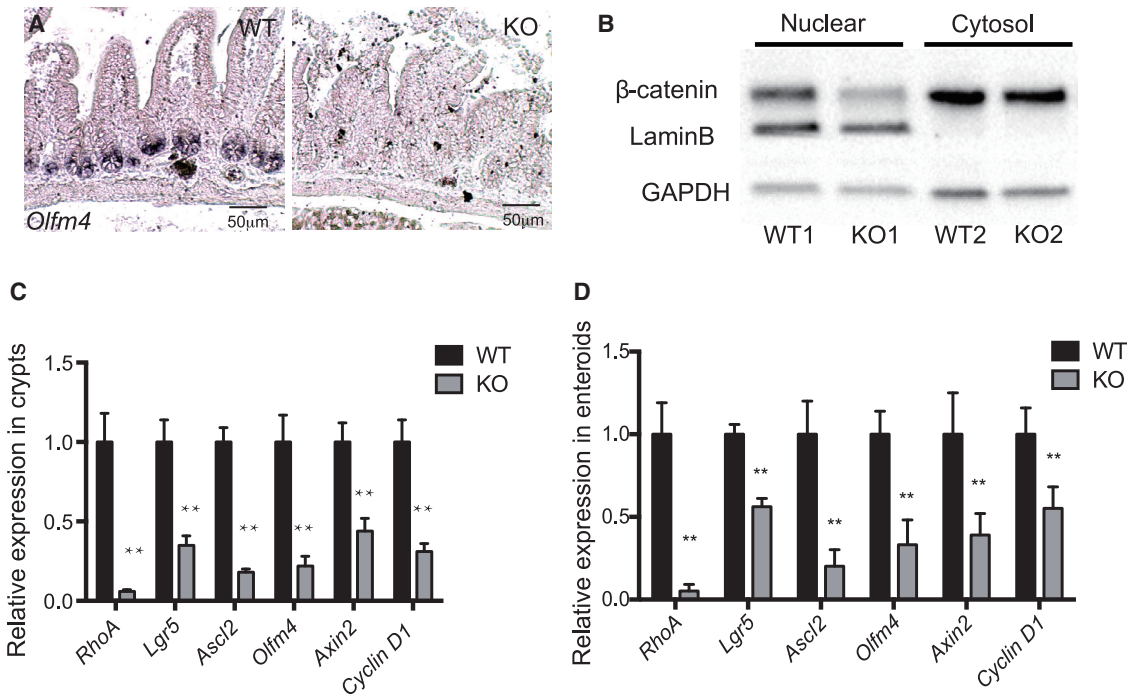

Figure 3. RhoA Deletion Leads to a Loss of Intestinal Stem Cells and Reduced Canonical Wnt Signaling *In Vivo* and *In Vitro*

(A) Representative images of *in situ* hybridization of *Olfm4* RNA in control WT and *RhoA* KO duodenum sections.

(B) Western blotting of cytosolic and nuclear fractions of β-catenin protein from control WT and *RhoA* KO duodenal crypts. GAPDH and laminin B protein expressions were used as controls for the cytosolic and nuclear fractions, respectively.

(C and D) qRT-PCR analysis of RNA expressions of ISC markers and Wnt target genes in isolated control WT and *RhoA* KO duodenal crypts (C) and enteroids (D). Data are normalized to GAPDH; n = 3 mice for each genotype. $^{**}p < 0.01$. Error bars represent SD from three independent experiments.

investigated the canonical Wnt signaling in *RhoA* KO crypts. A qRT-PCR analysis showed that the canonical Wnt pathway targets *Axin2* and *Cyclin D1* were both significantly reduced in the RHOA loss-of-function crypts (Figure 3C), suggesting impaired canonical Wnt signaling upon *RhoA* KO. Consistently, the protein level of nuclear β-catenin, as a readout of canonical Wnt signaling, was correspondingly reduced in *RhoA* KO crypts (Figure 3B).

To further examine whether RHOA regulates the function of ISCs, we performed an *in vitro* intestinal organoid (enteroid) culture assay using enteroids derived from Lgr5-EGFP-IRES-CreERT2; Villin-CreERT2;$RhoA^{fl/fl}$ (KO) and Lgr5-EGFP-IRES-CreERT2; Villin-CreERT2; $RhoA^{fl/+}$ mice (WT). Four days after culture, $Lgr5^{-}eGFP^{+}$ stem cells were localized at the tip of crypt-like intrusions surrounding the central lumen (green due to autofluorescence) lined by villus-like epithelium (Figure S4C). Consistent with the loss of ISC phenotype upon RHOA deletion *in vivo*, 4-OH tamoxifen-induced RHOA deletion *in vitro* inhibited the formation of crypt-like domains, leading to the loss of $Lgr5^{-}eGFP^{+}$ ISCs (Figure S4C). Addition of Y27632, an inhibitor of the major RHOA signaling effector ROCK, into the medium (for 4 days) phenocopied RHOA deletion, causing a loss of $Lgr5^{-}eGFP^{+}$ ISCs (Figure S4C). qRT-PCR performed 1 day after tamoxifen-induced RHOA deletion revealed a similar transcriptional reduction of ISC markers, i.e., *Lgr5*, *Ascl2*, and *Olfm4*, which is associated with a reduction of canonical Wnt markers *Axin2* and *Cyclin D1* in *RhoA* KO enteroids (Figure 3D). An examination of non-canonical Wnt antagonists *DKK1* and *Wnt5A* in WT and KO enteroids by qRT-PCR found their transcription levels very low and remained unchanged upon *RhoA* KO (data not shown). Together, these results suggest that RHOA signaling regulates ISC cell fate.

YAP Signaling Mediates the *RhoA* KO Phenotype of ISC Loss

The Hippo/YAP pathway has been reported as an important regulator during ISC regeneration (Barry and Camargo, 2013), and RHOA GTPases regulate YAP1 and TAZ transcriptional activities (Yu et al., 2012). To examine whether Hippo signaling is involved in the *RhoA* KO phenotypes, we first determined the expression of total YAP protein in

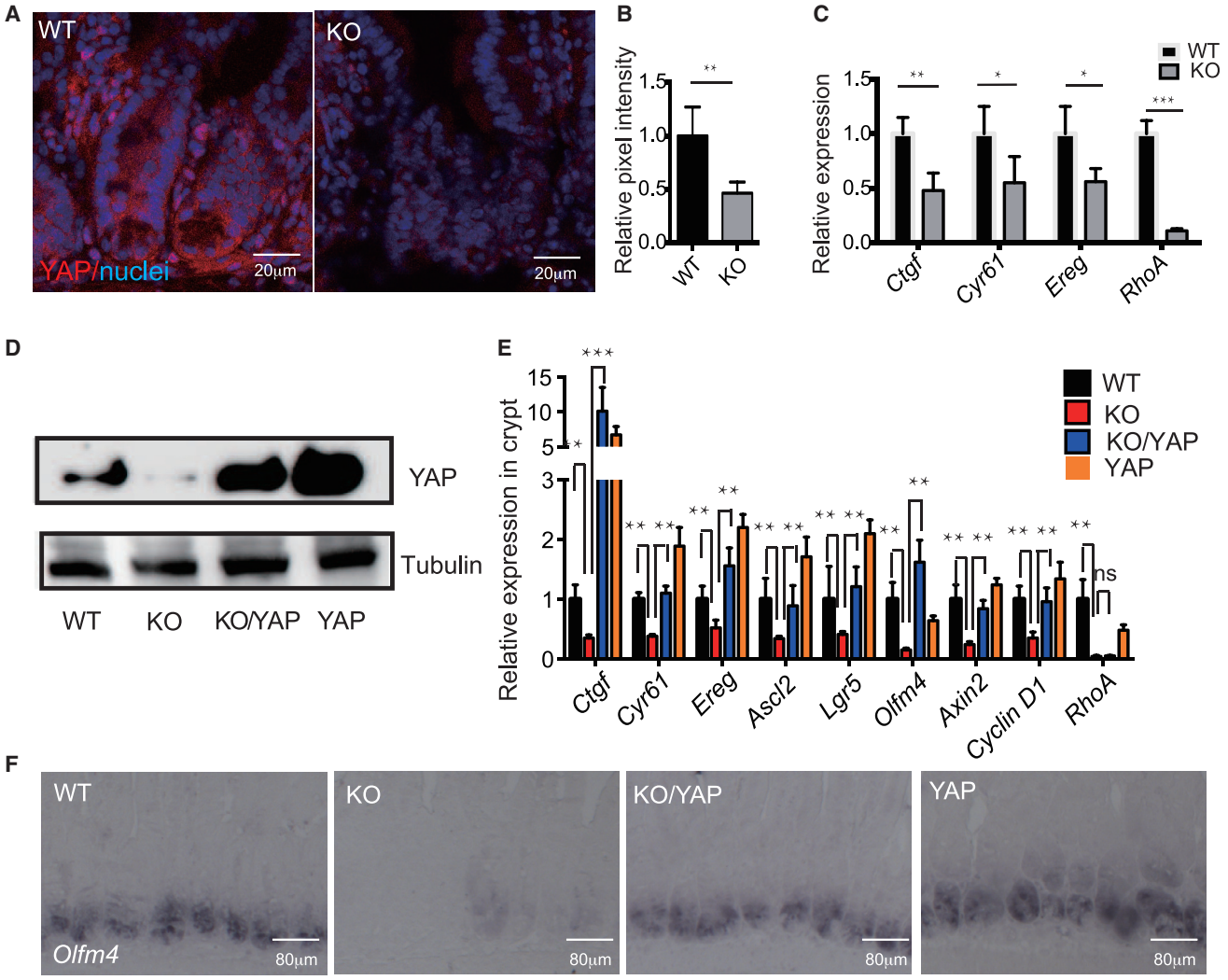

Figure 4. YAP Signaling Mediates the *RhoA* KO Phenotype of ISC Loss

(A) Representative immunofluorescence staining of total YAP in control and *RhoA* KO small intestine.

(B) Quantification of fluorescence intensity of nuclear YAP staining in control and *RhoA* KO crypts. Normalized to DAPI staining, n = 4 mice for each genotype. Error bars represent SD from three independent experiments.

(C) qRT-PCR showing expression of YAP signaling targets in control and *RhoA* KO duodenal crypts. Data are normalized to GAPDH expression; n = 3 mice for each genotype. Error bars represent SD from three independent experiments.

(D) Western blotting of total YAP protein using duodenal crypts isolated from control WT, *RhoA* KO, KO/*YAP* (S112A) rescue, and *YAP* (S112A) expressing enteroids.

(E) qRT-PCR analysis showing the expression of YAP transcriptional targets, ISC markers, and canonical Wnt signaling target genes in control WT, *RhoA* KO, KO/*YAP*(S112A) rescue, and *YAP*(S112A) expressing duodenal crypts. Data are normalized to GAPDH; n = 3 mice for each genotype. Error bars represent SD from three independent experiments.

(F) *In situ* hybridization analysis of *Olfm4* RNA in control WT, *RhoA* KO, KO/*YAP*(S112A) rescue, and *YAP*(S112A) expressing duodenum.

*p < 0.05, **p < 0.01, ***p < 0.001; ns, not significant.

the crypts by immunostaining. *RhoA* KO crypts exhibited significantly lower total YAP and nuclear YAP expressions, indicative of reduced YAP signaling activity (Figures 4A and 4B). Consistently, the transcripts of the YAP signaling targets, *Ctgf*, *Cyr61*, and *Ereg*, were repressed in *RhoA* KO crypts as well (Figure 4C), and western blotting of total YAP showed a significant reduction of YAP protein in *RhoA* KO crypts (Figure 4D).

To further determine whether YAP signaling plays a role in the RHOA-mediated ISC regulation, we took a genetic rescue approach to cross Villin-CreERT2; $RhoA^{fl/fl}$ (KO) mice or Villin-CreERT2; $RhoA^{fl/+}$ (WT) with mice expressing

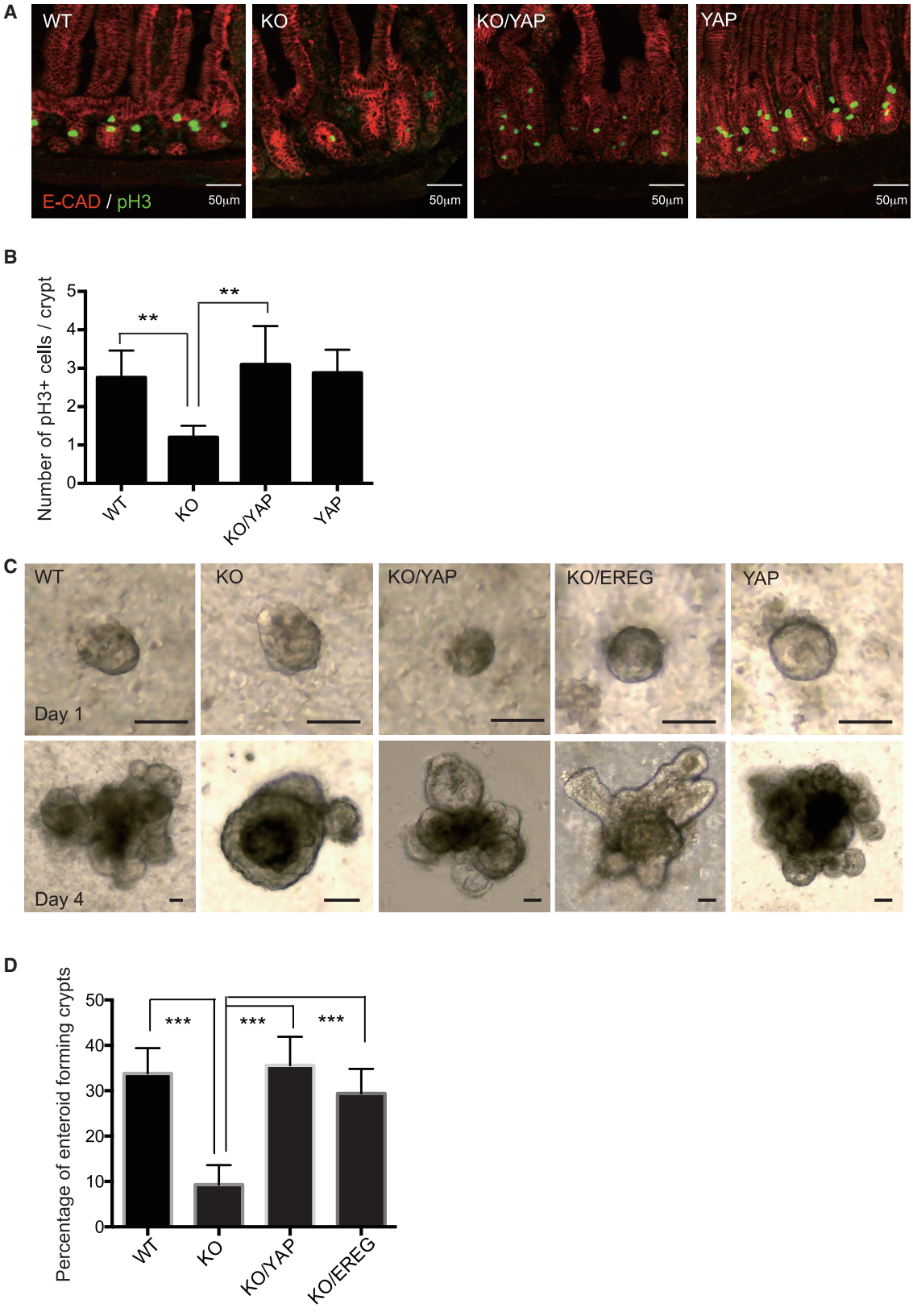

(legend on next page)

an inducible active *YAP* (S112A) mouse model, which turns on YAP nuclear activity upon Cre induction with tamoxifen. The active YAP mutant expression readily rescued the transcription of the YAP signaling targets, *Ctgf*, *Cyr61*, and *Ereg*, as well as the ISC markers, *Ascl2*, *Lgr5*, and *Olfm4*. Interestingly, canonical Wnt targets *Axin2* and *Cyclin D1* were also rescued by the active YAP mutant in *RhoA* KO (Figure 4E), consistent with a rescue of ISCs by the active YAP mutant signaling. An *in situ* hybridization with a probe against *Olfm4* confirmed that the active YAP mutant rescued the ISC marker expression in the *RhoA* KO (Figure 4F), while H&E staining showed that the active YAP mutant could not restore the disrupted villi structure (Figure S5A).

As *RhoA* KO has significantly reduced proliferation and disrupted structure in small intestinal epithelium, we tested whether active YAP is able to rescue the defects by immunostaining of pH3, E-cadherin, and β-catenin. The active YAP mutant rescued cell proliferation in the crypts, but not the disrupted epithelial organization (Figures 5A, 5B, and S5B). Surprisingly, we saw increased cytoplasmic YAP staining besides nuclear YAP in our YAP mutant rescue mice, which may be due to a compensatory reaction of the endogenous YAP (Figure S5B). We also used enteroid culture assays to determine the function of YAP signaling in ISC regeneration. In a 1-day culture, the isolated crypts of all genotypes formed similar small sphere-like enteroids; however, after 4 days in culture there was little budding or growth of the *RhoA* KO enteroids, and significantly fewer buds developed from *RhoA* KO enteroids compared with WT control (Figures 5C and 5D). Inducible expression of the active *YAP*(S112A) mutant, or an addition of the YAP target EREG protein to the culture medium, rescued enteroid-forming efficiency and enteroid growth (Figures 5C and 5D). These results indicate that YAP signaling mediates ISC homeostasis and regeneration under the RHOA null genetic conditions.

Constitutively Active β-Catenin Overcomes the Loss of ISC Phenotype in *RhoA* KO Crypts Independent of YAP Signaling

Since canonical Wnt signaling, known to be critical for ISC homeostasis and regeneration (Clevers, 2013; Reya and Clevers, 2005), is reduced in *RhoA* KO small intestinal crypts but can be rescued by active YAP mutant, we next tested the hypothesis that active canonical Wnt signaling may rescue ISC defects in *RhoA* KO mice. To this end, we crossed Villin-CreERT2; $RhoA^{fl/fl}$ (KO) mice or Villin-CreERT2; $RhoA^{fl/+}$ (WT) with $Catnb^{lox(ex3)}$ mice, which express an active β-catenin mutant upon Cre induction (Harada et al., 1999). H&E staining found that upon tamoxifen injection, Villin-CreERT2; $RhoA^{fl/fl}$; $Catnb^{lox(ex3)}$ mice (KO/β-Cat) showed a more organized crypt structure compared with the *RhoA* KO (Figure S6A), whereas Villin-CreERT2; $RhoA^{fl/+}$; $Catnb^{lox(ex3)}$ (β-Cat) mice had expanded crypts with large Paneth cells, consistent with canonical Wnt overexpression phenotype (Farin et al., 2012). *In situ* hybridization analysis of the ISC marker *Olfm4* showed that the Wnt activation by $Catnb^{lox(ex3)}$ expression rescued the loss of ISC phenotype of *RhoA* KO mice (Figure 6A), while β-Cat $Catnb^{lox(ex3)}$ mice displayed expanded *Olfm4* expressing crypts. Immunostaining of pH3 and E-cadherin suggested that active canonical Wnt signaling could rescue the proliferation defects in RHOA-depleted crypts, and the crypt/villi structures also seemed to be partially restored (Figures 6B and 6C). Finally, qRT-PCR analysis of ISC markers *Lgr5*, *Ascl2*, and *Olfm4* in isolated crypts further verified that expression of these markers in KO ISCs were restored by the active β-catenin expression (Figure 6D).

We further examined whether active canonical Wnt signaling is sufficient to rescue the *RhoA* KO ISC defects *in vitro*. Crypts from KO/β-Cat $Catnb^{lox(ex3)}$ mice formed enteroids that mimicked WT enteroids after a 4-day culture, with many buds forming in the enteroids, whereas the enteroids grown from β-Cat $Catnb^{lox(ex3)}$ mice formed a large balloon-like structure that is indicative of excessive Wnt activity (Figure 7A). qRT-PCR analysis of the enteroids showed similar results to that of *in vivo* analysis, i.e., the ISC markers *Lgr5*, *Ascl2*, and *Olfm4*, as well as the Wnt target *Axin2*, were readily rescued in KO/β-Cat $Catnb^{lox(ex3)}$ enteroids (Figure 7B). Interestingly, we found that active canonical Wnt signaling did not affect YAP signaling activity as assayed by a YAP transcription target gene analysis (Figure 7C) and YAP protein immunostaining (Figure S6B), suggesting that canonical Wnt-activity involved in ISC

Figure 5. YAP Signaling Rescues Proliferation and Enteroid Growth in *RhoA* KO

(A) Representative immunofluorescence staining of phosphor-histone H3 in control WT, *RhoA* KO, KO/*YAP* (S112A) rescue, and *YAP* (S112A) mice small intestine.

(B) Quantification of number of phosphor-histone H3-positive cells per crypt in control WT, *RhoA* KO, KO/*YAP* (S112A) rescue, and *YAP* (S112A) small intestine. n = 3 mice for each genotype. Error bars represent SD from three independent experiments.

(C) Representative images of growth of control WT, *RhoA* KO, KO/*YAP*(S112A) rescue, KO/EREG rescue (0.5 μg/mL), and *YAP*(S112A) expressing enteroids after 1 day and 4 days of culture.

(D) Percentage of enteroids developed from same number of crypts planted. n = 3 mice for each genotype. Error bars represent SD from three independent experiments.

**p < 0.01, ***p < 0.001.

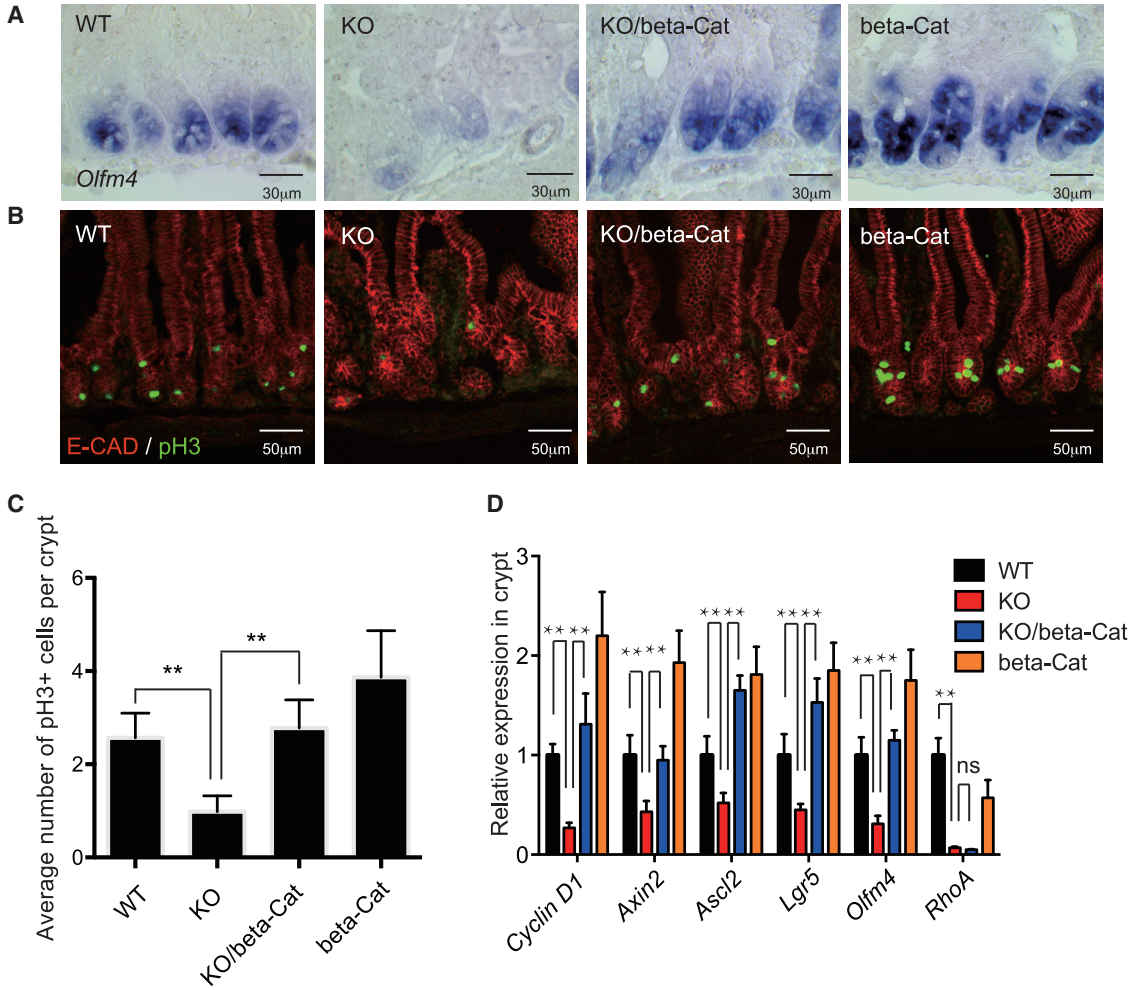

Figure 6. Constitutively Active β-Catenin Overcomes the Loss of ISC Phenotype in *RhoA* KO Crypts

(A) *In situ* hybridization of *Olfm4* RNA in control, *RhoA* KO, KO/β-catenin *Catnb*$^{lox(ex3)}$ rescue, and β-catenin *Catnb*$^{lox(ex3)}$ expressing duodenum.

(B) Representative immunofluorescence staining of phosphor-histone H3 in control WT, *RhoA* KO, KO/β-catenin *Catnb*$^{lox(ex3)}$ rescue, and β-catenin *Catnb*$^{lox(ex3)}$ expressing small intestine.

(C) Quantification of number of phosphor-histone H3-positive cells per crypt in control WT, *RhoA* KO, KO/β-catenin *Catnb*$^{lox(ex3)}$ rescue, and β-catenin *Catnb*$^{lox(ex3)}$ expressing small intestine. n = 3 mice for each genotype. Error bars represent SD from three independent experiments.

(D) qRT-PCR showing expression of ISCs markers and Wnt target genes in WT, *RhoA* KO, KO/β-catenin *Catnb*$^{lox(ex3)}$ rescue, and β-catenin *Catnb*$^{lox(ex3)}$ expressing crypts. Data are normalized to GAPDH expression; n = 3 mice for each genotype. Error bars represent SD from three independent experiments.

**p < 0.01; ns, not significant.

regeneration may function downstream of YAP signaling in the *RhoA* KO background.

DISCUSSION

As a founding member of the Rho GTPase family, RHOA regulates multiple important cellular functions including cytoskeleton dynamics, cell adhesion, survival, and cell cycle in various tissues (Zhou and Zheng, 2013), but little is known about its physiological function in small intestine in mammals. In this study, we utilize a genetic approach to inducibly and specifically delete RHOA in mouse small intestinal epithelium, and find that RHOA is essential for the maintenance of gut epithelial architecture and homeostasis of ISCs. Loss of RHOA causes a disrupted villi and

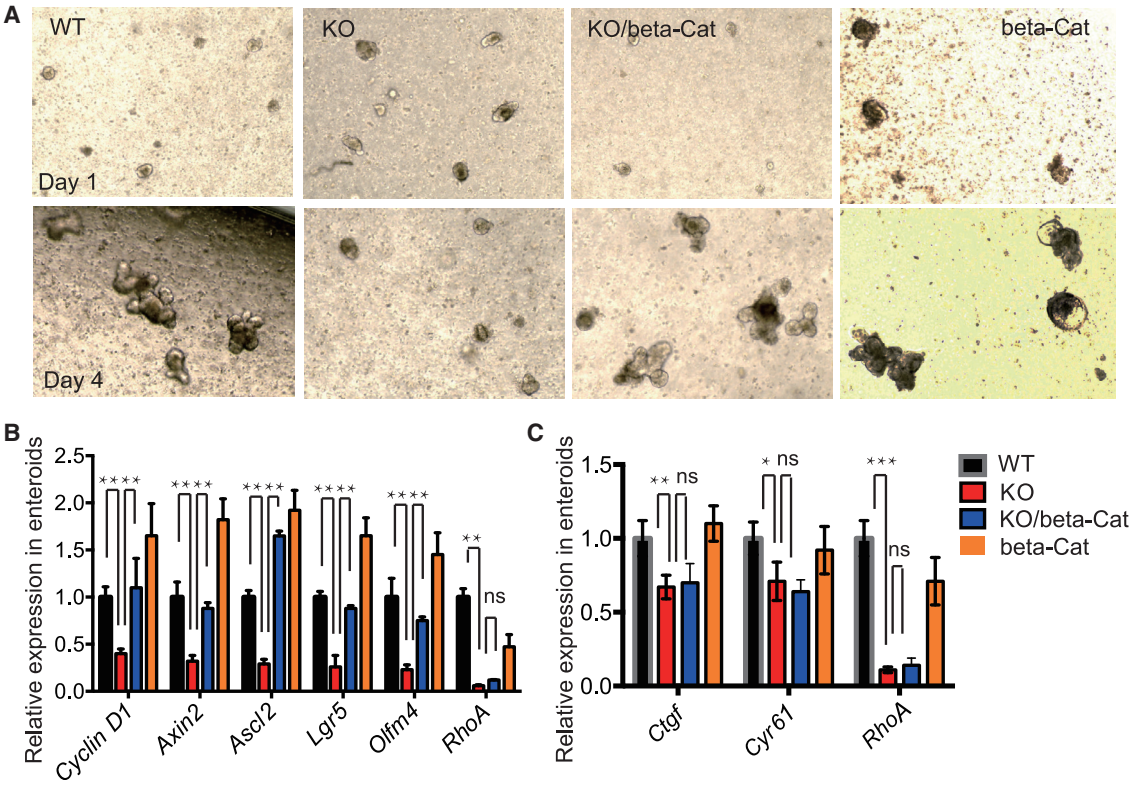

Figure 7. Constitutively Active β-Catenin Rescues *RhoA* KO Enteroid Growth Independent of YAP Signaling

(A) Representative images of WT, *RhoA* KO, KO/β-catenin *Catnb*$^{lox(ex3)}$ rescue, and β-catenin *Catnb*$^{lox(ex3)}$ expressing enteroids after 1 day and 4 days of culture.

(B and C) qRT-PCR showing expression of ISCs markers, Wnt target genes, YAP target genes in WT, *RhoA* KO, KO/β-catenin *Catnb*$^{lox(ex3)}$ rescue, and β-catenin *Catnb*$^{lox(ex3)}$ expressing enteroids. Data are normalized to GAPDH expression; n = 3 mice for each genotype. Error bars represent SD from three independent experiments.

*p < 0.05, **p < 0.01, ***p < 0.001; ns, not significant.

crypt structure in the small intestine, with defects in cell adhesion and junction. In addition, RHOA-depleted epithelium loses polarity organization and epithelial integrity.

Five days after the absence of RHOA, crypt cell proliferation is significantly reduced while apoptosis is elevated, along with a drastically decreased number of ISCs. This is consistent with a multitude of studies showing that RHOA positively regulates cell proliferation in several tissues (Melendez et al., 2011). These effects upon RHOA loss are reminiscent of certain stress conditions, such as irradiation. For example, mice treated with 10 Gy of radiation share a similar phenotype with RHOA loss-of-function mice, including disrupted villi, reduced proliferation, ectopic apoptosis, and repressed ISC marker expressions (Figure S7). Interestingly, most of our *RhoA* KO mice were able to recover from the induced changes in the small intestine and eventually survive, possibly due to adaptive compensations from other Rho family members such as RhoB and RhoC (data not shown). EREG from the surrounding stroma cells may also play a compensatory role, as previously reported in YAP-depleted intestines (Gregorieff et al., 2015). A recent report using a non-inducible RHOA loss-of-function model showed chronic intestinal inflammation (Lopez-Posadas et al., 2016), which is not observed in our transiently inducible *RhoA* KO mice, suggesting that RHOA may have different roles during embryonic and early postnatal stages versus adult stage, or the compensatory effects from *RhoA* KO differ in short-term versus long-term reactions.

In the intestine, YAP1 protein is enriched at the bottom of the crypt where the ISCs congregate (Cai et al., 2010; Camargo et al., 2007), and multiple loss-of-function studies have shown that YAP/TAZ promotes proliferation and regeneration of ISCs (Hong et al., 2016). However, there is conflicting evidence that intestine-specific induction of YAP1 would reduce ISC number, suggesting a growth-suppressive function of overexpressed YAP1 (Barry et al.,

2013). We find that YAP and its targets such as EREG are significantly reduced in *RhoA* KO crypts, and our genetic rescue experiment with a constitutively active form of YAP mutant can rescue ISC number and function of the KO mice, suggesting that YAP acts downstream of RHOA to positively regulate ISC regeneration. YAP and TAZ transcriptional activities can be regulated by multiple signals including mechanical stress, polarity, and Rho GTPases (Dupont et al., 2011; Rauskolb et al., 2014; Yu et al., 2012; Zhao et al., 2012); thus, possibly, RHOA-mediated epithelial polarity can regulate YAP/TAZ through Lats1/2 as previously reported (Yu et al., 2012).

Previous loss-of-function studies have found that YAP1 is dispensable during normal intestinal homeostasis, whereas it is essential for regeneration after irradiation injury (Gregorieff et al., 2015). Since *RhoA* KO shows multiple defects similar to those of irradiation-induced injuries, reduced YAP signaling in the *RhoA* KO could contribute to the defects in ISC regeneration as in the YAP-deleted intestine (Gregorieff et al., 2015). However, no reduced ISC number or ISC maker expression is observed in our YAP-overexpressing mice, differing from a previous report (Barry et al., 2013).

Wnt signaling is well established as being essential for the maintenance of the proliferative crypt compartment, and loss-of-function studies support the idea that the Wnt pathway constitutes the master regulator for intestinal homeostasis and maintenance of ISCs (Fevr et al., 2007; Korinek et al., 1998; Kuhnert et al., 2004; Pinto et al., 2003). However, the interaction between canonical Wnt and YAP signaling remains controversial, as some reports propose that YAP1 maintains the proliferation and function of ISCs by activating canonical Wnt signaling activity (Camargo et al., 2007) while others show that cytoplasmic YAP1 inhibits canonical Wnt signaling (Barry et al., 2013). Our study indicates that in the RHOA-depleted background, ectopic YAP activity promotes ISC regeneration and canonical Wnt signaling, while canonical Wnt signaling has no obvious impact on YAP signaling activity. How active YAP restores canonical Wnt signaling in *RhoA* KO small intestine needs further investigation, but it is not through a crosstalk with non-canonical Wnt signaling as previously reported in other model systems (Park et al., 2015), and may be via an indirect effect such that YAP, through EREG, restores the ISC proliferation and homeostasis that affects canonical Wnt activity. Our genetic rescue experiment with a stabilized β-catenin mutant suggests that canonical Wnt signaling is sufficient for ISC regeneration in the absence of RHOA and/or intact YAP signaling. This discovery implicates canonical Wnt signaling for small intestine regeneration after injury. However, exaggerated Wnt signaling can promote ISC hyperproliferation, and an optimal Wnt signaling dose needs to be precisely modulated for proper intestinal homeostasis (Clevers, 2013).

RHOA is a molecular switch in transducing diverse extracellular signals and is activated from a GDP-bound inactive form to a GTP-bound active form in response to stimuli (Etienne-Manneville and Hall, 2002; Karlsson et al., 2009; Liu et al., 2012; Wang and Zheng, 2007). The positive stimuli of RHOA include mechanical stress post injury (Aikawa et al., 1999; Smith et al., 2003), cytokines released due to inflammation (Campos et al., 2009; Iwata et al., 2012), and GPCRs hijacked in colon cancer conditions (Dorsam and Gutkind, 2007), which are involved in multiple disease states. Such altered pathophysiological status may regulate RHOA activity, which in turn affects ISCs. Further examination of how altered pathologic signals may be transduced through the identified RHOA-YAP-EREG pathway in intestinal diseases that result in altered ISC homeostasis will be of future interest.

EXPERIMENTAL PROCEDURES

Animal Studies

We used a $RhoA^{lox/flox}$ mouse line described previously (Katayama et al., 2011). The $RhoA^{flox/flox}$ mouse was crossed with Villin-$CreER^{T2}$ mice provided by Dr. Helen Piwnica-Worms at the University of Texas MD Anderson Center. Littermate controls were generated by standard pairings. Animal protocols were approved by the Cincinnati Children's Hospital Medical Center Committee on the Ethics of Animal Experiments. All mice were housed in a specific pathogen-free breeding barrier. Euthanasia was performed by CO_2 followed by cervical dislocation. To induce Cre recombinase, we intraperitoneally injected 6- to 8-week-old adult mice with 1 mg of tamoxifen (Sigma-Aldrich, Switzerland) dissolved in corn oil for 4 consecutive days. Mice were euthanized and analyzed 1 day after the last injection. For the genetic rescue experiment, we crossed $RhoA^{flox/flox}$; Villin-$CreER^{T2}$ mice (Melendez et al., 2011) to knockin mice containing either an inducible active YAP mutant allele (S112A mutation [Xin et al., 2011], under the control of CMV-LSL) or an inducible active β-catenin mutant allele $catnb^{lox(ex3)}$ (Harada et al., 1999).

H&E Staining and Tissue Preparation

Intestinal tissues were flushed with PBS and fixed in 10% formalin or 4% paraformaldehyde overnight at 4°C. Tissues were then embedded in paraffin or cold optimum cutting temperature (OCT) embedding medium. Processing of tissues for paraffin embedding and H&E staining was performed by the CCHMC Digestive Health Center Morphology Core.

Immunofluorescence and Confocal Microscopy

Immunofluorescence was performed on frozen sections. Intestinal tissues were flushed with PBS and fixed in 4% paraformaldehyde overnight at 4°C, cryoprotected in 30% sucrose, embedded in OCT compound, and sectioned at 12 μm. Antibodies for immunofluorescence are: RHOA (Cell Signaling Technology, #2117, 1:250),

cleaved caspase-3 (Cell Signaling, #9661, 1:250), p-histone H3 (Cell Signaling, #9701, 1:250), laminin B (Cell Signaling, #12586, 1:250), E-cadherin (BD Biosciences, #610181, 1:250), β-catenin (BD Biosciences, #610153, 1:250), Na^+,K^+-ATPase α (MBL, #D154-3, 1:250), Ki67 (Abcam, #ab15580, 1:200), chromogranin A (Abcam, # ab15160, 1:200), lysozyme (Dako, #A0099, 1:2000), and mucin-2 (Thermo Scientific, #MS-1037, 1:200).

Images were acquired on a Zeiss 710 and Nikon A1R GaAsP Inverted Confocal Microscope. Signal intensity was optimized for control samples and the same settings (laser power/gain/offset) were used for *RhoA* KO tissue and cells. Phase-contrast images of enteroids were captured on an Olympus IX51 microscope equipped with a Q Color 5 camera and acquired with Q Capture Pro 6.0 software.

In Situ Hybridization

Intestinal tissues were flushed with PBS and fixed in 10% formalin or 4% paraformaldehyde overnight at 4°C. Tissues were then embedded in paraffin or cold OCT embedding medium. Processing of tissues for paraffin embedding was performed by the CCHMC Digestive Health Center Morphology Core, and *in situ* hybridization was performed following a published protocol (Gregorieff and Clevers, 2010).

Western Blotting

Intestinal epithelium from villi and crypts were isolated as previously described (Melendez et al., 2013). Tissues were homogenized in lysis buffer containing protease and phosphatase inhibitors, sonicated at 4°C, mixed with 4× SDS loading buffer, and heated at 100°C for 5 min. A Bradford assay was used to determine protein concentration (Bio-Rad). Antibodies for western blotting are: anti-RHOA (#2117), Cdc42 (#2462), MLC2 (#3671), p-MLC2 (#3675), Bcl-2 (#15071), BCL-xL (#2764), p53 (#2527), p-p53 (#2521), cleaved caspase-3 (#9661), YAP (#14074), and GAPDH (#5174) (all from Cell Signaling), and anti-Rac1 antibody (#610650, BD Biosciences). The FOCUS SubCell kit (G Biosciences) was used to separate crypt cell cytosolic and nuclear fractions.

Transmission Electron Microscopy

For transmission electron microscopy, small intestinal sections were dissected, flushed with cold PBS supplemented with protease inhibitors, and fixed in 4% glutaraldehyde/0.175 M cacodylate buffer followed by 1% osmium tetroxide/0.175 M cacodylate. Mouse tissues were then dehydrated, embedded in LX-112 resin, and imaged by the CCHMC Digestive Health Center Morphology Core.

RNA Extraction and Real-Time qPCR

mRNA was isolated from intestinal crypts using an RNA Mini Kit (Qiagen). RNA concentration was measured by Nanodrop and cDNA was produced with a cDNA synthesis kit (ABI). qPCR was performed using SYBR qPCR master mix (ABI) or TaqMan qPCR master mix (ABI) on an ABI700 qRT-PCR instrument. Relative expression levels were determined by the ΔΔCt method standardized to *gapdh*. Primer sequences for SYBR reaction were obtained from web source http://medgen.ugent.be/rtprimerdb or http://pga.mgh.harvard.edu/primerbank (see below for sequences).

SYBR Reaction qRT-PCR Primer Sequences

Bmi1: 5′-CAC CCA CAG TTC CCT CAC ATT-3′ and 5′-TCG AGG TCT ACT GGC AAA GGA-3′

Axin2: 5′-GTG GAT ACG CTG GAC TTC TGG-3′ and 5′-GAG CCG ATC TGT TGC TTC TTG-3′

Cyclin D 1: 5′-GTG AGG GAA GAG GTG AAG GTG-3′ and 5′-GAT CCT GGG AGT CAT CGG TAG-3′

E-cadherin: 5′-CAC CTG GAG AGA GGC CAT GT-3′ and 5′-TGG GAA ACA TGA GCA GCT CT-3′

B-*catenin*: 5′-ATG GAG CCG GAC AGA AAA GC-3′ and 5′-CTT GCC ACT CAG GGA AGG A-3′

Par3: 5′-CAC CAT GCG GAA GAT GAT CTG-3′ and 5′-GAG CCG TTT TTA TTG CAC ACC-3′

Par6: 5′-TCT GTA CGG GTG CAT GTT CAG-3′ and 5′-TGC CAG GTT AAT CAT GTA CGT TG-3′

Zo-1: 5′-GAA CCA ATT CGC CGA GAA GG-3′ and 5′-CTG TTG CCC GCA TGT GAT G-3′

Gapdh: H: 5′-CGT ATT GGG CGC CTG GTC AC-3′ and 5′-ATG ATG ACC CTT TTG GCT CC-3′

TaqMan reaction qRT-PCR primer item number (Thermo Fisher)

Ctgf: Mm01192933_g1; *Cyr61*: Mm00487499_g1;

Ereg: Mm00514794_m1; *RhoA*: Mm00834507_g1;

Lgr5: Mm00438890_m1; *Olfm4*: Mm01320260_m1;

Ascl2: Mm01268891_g1.

RhoA-Inducible Deletion in Enteroid Culture and Staining

Duodenal crypts from 6- to 8-week old control and *RhoA* KO mice were isolated and cultured *in vitro* as previously described (Mahe et al., 2013; Sato et al., 2011; Snippert et al., 2010). At 24 hr post passage, RHOA deletion was induced with 1 μM 4-OHT and complete deletion of *RhoA* allele was observed after 48 hr and detected by genomic PCR. At 5–7 days post induction, enteroids were fixed in 4% paraformaldehyde for 1.5 hr at room temperature and then washed in TBS/0.3% Tween 20. Fixed enteroids were blocked for 3 hr at room temperature in 2% normal goat serum/4% BSA/TBS/0.1% Tween 20, followed by an antibody.

Detailed protocols of quantification of Paneth cells, Goblet cells, and enteroendocrine cells are described elsewhere (Melendez et al., 2013).

Quantification

Paneth cell number was quantified by counting the average number of lysosome-positive cells in crypts and villi (50 crypts and villi per mouse). Nuclear YAP signaling was quantified by measuring the YAP immunostaining intensity using ImageJ, which is normalized to DAPI nuclei staining (50 crypts per mouse).

Statistics

Results are expressed as the mean ± SD. Significance was calculated by Student's t test. $p < 0.05$ was considered significant.

SUPPLEMENTAL INFORMATION

Supplemental Information includes seven figures and can be found with this article online at https://doi.org/10.1016/j.stemcr.2017.10.004.

AUTHOR CONTRIBUTIONS

M.L., Z.Z., L.S., X.Z., and Y.Z. designed the study and developed the methodologies. M.L., Z.Z., L.S., X.Z., Y.F., S.A., J.M., A.K.D, F.B., and M.X. collected data, performed the analysis, and contributed critical reagents. K.N. and H.G. contributed critical reagents and technical expertise. M.L., Z.Z., and Y.Z. wrote the manuscript.

ACKNOWLEDGMENT

This work was in part supported by NIH grants R01 DK104814, R01 HL134617, R01 CA193350, and P30 DK078392 (Pathology Core).

Received: July 2, 2017
Revised: October 10, 2017
Accepted: October 11, 2017
Published: November 9, 2017

REFERENCES

Aikawa, R., Komuro, I., Yamazaki, T., Zou, Y., Kudoh, S., Zhu, W., Kadowaki, T., and Yazaki, Y. (1999). Rho family small G proteins play critical roles in mechanical stress-induced hypertrophic responses in cardiac myocytes. Circ. Res. *84*, 458–466.

Azzolin, L., Panciera, T., Soligo, S., Enzo, E., Bicciato, S., Dupont, S., Bresolin, S., Frasson, C., Basso, G., Guzzardo, V., et al. (2014). YAP/TAZ incorporation in the beta-catenin destruction complex orchestrates the Wnt response. Cell *158*, 157–170.

Barker, N., and Clevers, H. (2010). Leucine-rich repeat-containing G-protein-coupled receptors as markers of adult stem cells. Gastroenterology *138*, 1681–1696.

Barker, N., van Es, J.H., Kuipers, J., Kujala, P., van den Born, M., Cozijnsen, M., Haegebarth, A., Korving, J., Begthel, H., Peters, P.J., et al. (2007). Identification of stem cells in small intestine and colon by marker gene Lgr5. Nature *449*, 1003–1007.

Barry, E.R., and Camargo, F.D. (2013). The Hippo superhighway: signaling crossroads converging on the Hippo/Yap pathway in stem cells and development. Curr. Opin. Cell Biol. *25*, 247–253.

Barry, E.R., Morikawa, T., Butler, B.L., Shrestha, K., de la Rosa, R., Yan, K.S., Fuchs, C.S., Magness, S.T., Smits, R., Ogino, S., et al. (2013). Restriction of intestinal stem cell expansion and the regenerative response by YAP. Nature *493*, 106–110.

Benoit, Y.D., Lussier, C., Ducharme, P.A., Sivret, S., Schnapp, L.M., Basora, N., and Beaulieu, J.F. (2009). Integrin alpha8beta1 regulates adhesion, migration and proliferation of human intestinal crypt cells via a predominant RhoA/ROCK-dependent mechanism. Biol. Cell *101*, 695–708.

Cai, J., Maitra, A., Anders, R.A., Taketo, M.M., and Pan, D. (2015). beta-Catenin destruction complex-independent regulation of Hippo-YAP signaling by APC in intestinal tumorigenesis. Genes Dev. *29*, 1493–1506.

Cai, J., Zhang, N., Zheng, Y., de Wilde, R.F., Maitra, A., and Pan, D. (2010). The Hippo signaling pathway restricts the oncogenic potential of an intestinal regeneration program. Genes Dev. *24*, 2383–2388.

Camargo, F.D., Gokhale, S., Johnnidis, J.B., Fu, D., Bell, G.W., Jaenisch, R., and Brummelkamp, T.R. (2007). YAP1 increases organ size and expands undifferentiated progenitor cells. Curr. Biol. *17*, 2054–2060.

Campos, S.B., Ashworth, S.L., Wean, S., Hosford, M., Sandoval, R.M., Hallett, M.A., Atkinson, S.J., and Molitoris, B.A. (2009). Cytokine-induced F-actin reorganization in endothelial cells involves RhoA activation. Am. J. Physiol. Ren. Physiol. *296*, F487–F495.

Cheng, H., and Leblond, C.P. (1974). Origin, differentiation and renewal of the four main epithelial cell types in the mouse small intestine. V. Unitarian Theory of the origin of the four epithelial cell types. Am. J. Anat. *141*, 537–561.

Clevers, H. (2013). The intestinal crypt, a prototype stem cell compartment. Cell *154*, 274–284.

Dorsam, R.T., and Gutkind, J.S. (2007). G-protein-coupled receptors and cancer. Nat. Rev. Cancer *7*, 79–94.

Dupont, S., Morsut, L., Aragona, M., Enzo, E., Giulitti, S., Cordenonsi, M., Zanconato, F., Le Digabel, J., Forcato, M., Bicciato, S., et al. (2011). Role of YAP/TAZ in mechanotransduction. Nature *474*, 179–183.

Etienne-Manneville, S., and Hall, A. (2002). Rho GTPases in cell biology. Nature *420*, 629–635.

Farin, H.F., Van Es, J.H., and Clevers, H. (2012). Redundant sources of Wnt regulate intestinal stem cells and promote formation of Paneth cells. Gastroenterology *143*, 1518–1529.e7.

Fevr, T., Robine, S., Louvard, D., and Huelsken, J. (2007). Wnt/beta-catenin is essential for intestinal homeostasis and maintenance of intestinal stem cells. Mol. Cell Biol. *27*, 7551–7559.

Gregorieff, A., and Clevers, H. (2010). In situ hybridization to identify gut stem cells. Curr. Protoc. Stem Cell Biol. *Chapter 2*, Unit 2F.1.

Gregorieff, A., Liu, Y., Inanlou, M.R., Khomchuk, Y., and Wrana, J.L. (2015). Yap-dependent reprogramming of Lgr5(+) stem cells drives intestinal regeneration and cancer. Nature *526*, 715–718.

Harada, N., Tamai, Y., Ishikawa, T., Sauer, B., Takaku, K., Oshima, M., and Taketo, M.M. (1999). Intestinal polyposis in mice with a dominant stable mutation of the beta-catenin gene. EMBO J. *18*, 5931–5942.

Hong, A.W., Meng, Z., and Guan, K.L. (2016). The Hippo pathway in intestinal regeneration and disease. Nat. Rev. Gastroenterol. Hepatol. *13*, 324–337.

Imajo, M., Ebisuya, M., and Nishida, E. (2015). Dual role of YAP and TAZ in renewal of the intestinal epithelium. Nat. Cell Biol. *17*, 7–19.

Imajo, M., Miyatake, K., Iimura, A., Miyamoto, A., and Nishida, E. (2012). A molecular mechanism that links Hippo signalling to the inhibition of Wnt/beta-catenin signalling. EMBO J. *31*, 1109–1122.

Iwata, A., Shirai, R., Ishii, H., Kushima, H., Otani, S., Hashinaga, K., Umeki, K., Kishi, K., Tokimatsu, I., Hiramatsu, K., et al. (2012). Inhibitory effect of statins on inflammatory cytokine production from human bronchial epithelial cells. Clin. Exp. Immunol. *168*, 234–240.

Jackson, B., Peyrollier, K., Pedersen, E., Basse, A., Karlsson, R., Wang, Z., Lefever, T., Ochsenbein, A.M., Schmidt, G., Aktories, K., et al. (2011). RhoA is dispensable for skin development, but

crucial for contraction and directed migration of keratinocytes. Mol. Biol. Cell *22*, 593–605.

Kaibuchi, K., Kuroda, S., and Amano, M. (1999). Regulation of the cytoskeleton and cell adhesion by the Rho family GTPases in mammalian cells. Annu. Rev. Biochem. *68*, 459–486.

Karlsson, R., Pedersen, E.D., Wang, Z., and Brakebusch, C. (2009). Rho GTPase function in tumorigenesis. Biochim. Biophys. Acta *1796*, 91–98.

Katayama, K., Melendez, J., Baumann, J.M., Leslie, J.R., Chauhan, B.K., Nemkul, N., Lang, R.A., Kuan, C.Y., Zheng, Y., and Yoshida, Y. (2011). Loss of RhoA in neural progenitor cells causes the disruption of adherens junctions and hyperproliferation. Proc. Natl. Acad. Sci. USA *108*, 7607–7612.

Korinek, V., Barker, N., Moerer, P., van Donselaar, E., Huls, G., Peters, P.J., and Clevers, H. (1998). Depletion of epithelial stem-cell compartments in the small intestine of mice lacking Tcf-4. Nat. Genet. *19*, 379–383.

Kuhnert, F., Davis, C.R., Wang, H.T., Chu, P., Lee, M., Yuan, J., Nusse, R., and Kuo, C.J. (2004). Essential requirement for Wnt signaling in proliferation of adult small intestine and colon revealed by adenoviral expression of Dickkopf-1. Proc. Natl. Acad. Sci. USA *101*, 266–271.

Liu, M., Bi, F., Zhou, X., and Zheng, Y. (2012). Rho GTPase regulation by miRNAs and covalent modifications. Trends Cell Biol. *22*, 365–373.

Lopez-Posadas, R., Becker, C., Gunther, C., Tenzer, S., Amann, K., Billmeier, U., Atreya, R., Fiorino, G., Vetrano, S., Danese, S., et al. (2016). Rho-A prenylation and signaling link epithelial homeostasis to intestinal inflammation. J. Clin. Invest. *126*, 611–626.

Mahe, M.M., Aihara, E., Schumacher, M.A., Zavros, Y., Montrose, M.H., Helmrath, M.A., Sato, T., and Shroyer, N.F. (2013). Establishment of gastrointestinal epithelial organoids. Curr. Protoc. Mouse Biol. *3*, 217–240.

Melendez, J., Liu, M., Sampson, L., Akunuru, S., Han, X., Vallance, J., Witte, D., Shroyer, N., and Zheng, Y. (2013). Cdc42 coordinates proliferation, polarity, migration, and differentiation of small intestinal epithelial cells in mice. Gastroenterology *145*, 808–819.

Melendez, J., Stengel, K., Zhou, X., Chauhan, B.K., Debidda, M., Andreassen, P., Lang, R.A., and Zheng, Y. (2011). RhoA GTPase is dispensable for actomyosin regulation but is essential for mitosis in primary mouse embryonic fibroblasts. J. Biol. Chem. *286*, 15132–15137.

Park, H.W., Kim, Y.C., Yu, B., Moroishi, T., Mo, J.S., Plouffe, S.W., Meng, Z., Lin, K.C., Yu, F.X., Alexander, C.M., et al. (2015). Alternative Wnt signaling activates YAP/TAZ. Cell *162*, 780–794.

Pinto, D., Gregorieff, A., Begthel, H., and Clevers, H. (2003). Canonical Wnt signals are essential for homeostasis of the intestinal epithelium. Genes Dev. *17*, 1709–1713.

Rajasekaran, S.A., Palmer, L.G., Moon, S.Y., Peralta Soler, A., Apodaca, G.L., Harper, J.F., Zheng, Y., and Rajasekaran, A.K. (2001). Na,K-ATPase activity is required for formation of tight junctions, desmosomes, and induction of polarity in epithelial cells. Mol. Biol. Cell *12*, 3717–3732.

Rauskolb, C., Sun, S., Sun, G., Pan, Y., and Irvine, K.D. (2014). Cytoskeletal tension inhibits Hippo signaling through an Ajuba-Warts complex. Cell *158*, 143–156.

Reya, T., and Clevers, H. (2005). Wnt signalling in stem cells and cancer. Nature *434*, 843–850.

Rosenbluh, J., Nijhawan, D., Cox, A.G., Li, X., Neal, J.T., Schafer, E.J., Zack, T.I., Wang, X., Tsherniak, A., Schinzel, A.C., et al. (2012). beta-Catenin-driven cancers require a YAP1 transcriptional complex for survival and tumorigenesis. Cell *151*, 1457–1473.

Sato, T., and Clevers, H. (2013). Growing self-organizing mini-guts from a single intestinal stem cell: mechanism and applications. Science *340*, 1190–1194.

Sato, T., van Es, J.H., Snippert, H.J., Stange, D.E., Vries, R.G., van den Born, M., Barker, N., Shroyer, N.F., van de Wetering, M., and Clevers, H. (2011). Paneth cells constitute the niche for Lgr5 stem cells in intestinal crypts. Nature *469*, 415–418.

Sato, T., Vries, R.G., Snippert, H.J., van de Wetering, M., Barker, N., Stange, D.E., van Es, J.H., Abo, A., Kujala, P., Peters, P.J., et al. (2009). Single Lgr5 stem cells build crypt-villus structures in vitro without a mesenchymal niche. Nature *459*, 262–265.

Smith, P.G., Roy, C., Zhang, Y.N., and Chauduri, S. (2003). Mechanical stress increases RhoA activation in airway smooth muscle cells. Am. J. Respir. Cell Mol. Biol. *28*, 436–442.

Snippert, H.J., van der Flier, L.G., Sato, T., van Es, J.H., van den Born, M., Kroon-Veenboer, C., Barker, N., Klein, A.M., van Rheenen, J., Simons, B.D., et al. (2010). Intestinal crypt homeostasis results from neutral competition between symmetrically dividing Lgr5 stem cells. Cell *143*, 134–144.

Taniguchi, K., Wu, L.W., Grivennikov, S.I., de Jong, P.R., Lian, I., Yu, F.X., Wang, K., Ho, S.B., Boland, B.S., Chang, J.T., et al. (2015). A gp130-Src-YAP module links inflammation to epithelial regeneration. Nature *519*, 57–62.

Tian, H., Biehs, B., Chiu, C., Siebel, C.W., Wu, Y., Costa, M., de Sauvage, F.J., and Klein, O.D. (2015). Opposing activities of Notch and Wnt signaling regulate intestinal stem cells and gut homeostasis. Cell Rep. *11*, 33–42.

van der Flier, L.G., and Clevers, H. (2009). Stem cells, self-renewal, and differentiation in the intestinal epithelium. Annu. Rev. Physiol. *71*, 241–260.

van der Flier, L.G., Haegebarth, A., Stange, D.E., van de Wetering, M., and Clevers, H. (2009). OLFM4 is a robust marker for stem cells in human intestine and marks a subset of colorectal cancer cells. Gastroenterology *137*, 15–17.

Wang, L., and Zheng, Y. (2007). Cell type-specific functions of Rho GTPases revealed by gene targeting in mice. Trends Cell Biol. *17*, 58–64.

Xin, M., Kim, Y., Sutherland, L.B., Qi, X., McAnally, J., Schwartz, R.J., Richardson, J.A., Bassel-Duby, R., and Olson, E.N. (2011). Regulation of insulin-like growth factor signaling by Yap governs cardiomyocyte proliferation and embryonic heart size. Sci. Signal. *4*, ra70.

Yu, F.X., Zhao, B., Panupinthu, N., Jewell, J.L., Lian, I., Wang, L.H., Zhao, J., Yuan, H., Tumaneng, K., Li, H., et al. (2012). Regulation of the Hippo-YAP pathway by G-protein-coupled receptor signaling. Cell *150*, 780–791.

Zhao, B., Li, L., Lei, Q., and Guan, K.L. (2010). The Hippo-YAP pathway in organ size control and tumorigenesis: an updated version. Genes Dev. *24*, 862–874.

Zhao, B., Li, L., Wang, L., Wang, C.Y., Yu, J., and Guan, K.L. (2012). Cell detachment activates the Hippo pathway via cytoskeleton reorganization to induce anoikis. Genes Dev. *26*, 54–68.

Zhou, X., and Zheng, Y. (2013). Cell type-specific signaling function of RhoA GTPase: lessons from mouse gene targeting. J. Biol. Chem. *288*, 36179–36188.

Zhou, X., Florian, M.C., Arumugam, P., Chen, X., Cancelas, J.A., Lang, R., Malik, P., Geiger, H., and Zheng, Y. (2013). RhoA GTPase controls mitosis and programmed necrosis of hematopoietic progenitors. J. Exp. Med. *210*, 2371–2385.

Stem Cell Reports, Volume *9*

Supplemental Information

RHOA GTPase Controls YAP-Mediated EREG Signaling in Small Intestinal Stem Cell Maintenance

Ming Liu, Zheng Zhang, Leesa Sampson, Xuan Zhou, Kodandaramireddy Nalapareddy, Yuxin Feng, Shailaja Akunuru, Jaime Melendez, Ashley Kuenzi Davis, Feng Bi, Hartmut Geiger, Mei Xin, and Yi Zheng

Supplemental Figure Legends

Supplemental Figure 1. (Related to Figure 1) Expression of RhoA protein in small intestine and ISCs and genotyping of rhoA in villin-CreERT2+; RhoA flox/flox and control WT mice. (A-B) Representative immunofluorescent imaging of anti-RhoA, DAPI and Lgr5-eGFP in WTmouse small intestine at a magnification of 20X (A) or 63x (B). (C) Purified genomic DNAs isolated from small intestines of villin-CreERT2+; RhoA flox/flox mice and controls were subject to PCR genotyping as described in Methods to identify RhoA flox/flox and CreERT2+ alleles. (D) Genomic DNA samples of small intestine duodelum, jejunum and ileum were processed for PCR genotyping as described in Methods to identify RhoA deletion.

Supplemental Figure 2. (Related to Figure 1) Morphologic changes of RhoA knockout small intestines. (A) TEM analysis of the epithelium in control WT and RhoA KO small intestine sections. The EM image shows a disorganization of the epithelium structure and nuclear organization in RhoA KO small intestine epithelium. (B,C) The histology of different regions of small intestine in control WT and RhoA KO mice. Representative H&E staining shows the disrupted jejunum and ileum, particularly the crypts, in RhoA KO mice.

Supplemental Figure 3. (Related to Figure 2) Analyses of Goblet cells, enteroendocrine cells, Paneth cells multinucleated cells and proliferating cells in RhoA KO duodenum. Representative immunofluorescence images of Mucin-2 (A), chromogranin A (B), laminin B/E-Cad (C), cleaved caspase-3 (D), phospho-histone H3 (E) and lysosome (F, G) distributions in Control WT and RhoA KO small intestines.

Supplemental Figure 4. (Related to Figure 3) Analysis of ISCs in vivo and in vitro. (A) Direct fluorescence detection of Lgr5-EGFP signal in Control WT and RhoA KO duodenum sections. (B) Induced RhoA deletion in vitro causes a defective E-cadherin distribution in enteroid culture. Enteroids at day five post-induction by the addition of 4-OHT. Enteroids were stained with anti-RhoA (red) and anti-E-cadherin (green). (C) Direct fluorescence imaging of the Lgr5-EGFP signal (arrow head) from cultured enteroids

derived from Lgr5-EGFP-IRES-Cre-ERT2;Villin-CreERT2;rhoAfl/+ (WT) or Lgr5-EGFP-IRES-Cre-ERT2;Villin-CreERT2;rhoAfl/fl mice (KO), and the ROCK inhibitor Y27632 (10 μM) treated control.

Supplemental Figure 5. (Related to Figures 4 & 5) Rescue of RhoA KO phenotypes by an active YAP transgenic mutant. (A) The representative H&E staining images of Control WT, RhoA KO, KO/YAP (S112A) mutant and YAP (S112A) mutant small intestine duodenum. n=3 mice for each genotype. (B) Representative immunofluorescence staining of total YAP showing constitutively active YAP increase YAP protein level. (C) Representative immunofluorescence staining of beta-catenin showing constitutively active YAP does not impact membrane beta-catenin expression.

Supplemental Figure 6. (Related to Figures 6 & 7) Rescue of RhoA KO phenotypes by an active beta-catenin mutant. (A) H&E staining of Control WT, RhoA KO, KO/beta-catenin Catnblox(ex3) rescue and beta-catenin Catnblox(ex3) expressing duedenum. (B) Representative immunofluorescence staining of YAP showing beta-catenin Catnblox(ex3) does not impact YAP expression.

Supplemental Figure 7. (Related to Discussion) RhoA KO defects in small intestine in part mimic that of X-ray irradiation injuries. (A) H&E staining of Control WT and irradiated Control WT (IR) small intestine sections. (B-D) Representative immunofluorescence images of anti-E-cadherin, Ki-67, cleaved caspase 3 and lysozyme in Control, IR small intestine duodenum sections. (E) qRT-PCR analysis of the expression of ISC markers in WT and WT+ IR small intestinal crypts. Open bar, WT; black bar, WT + IR. Results are normalized to GAPDH expression and expressed as fold changes. n=3 mice for each genotype.

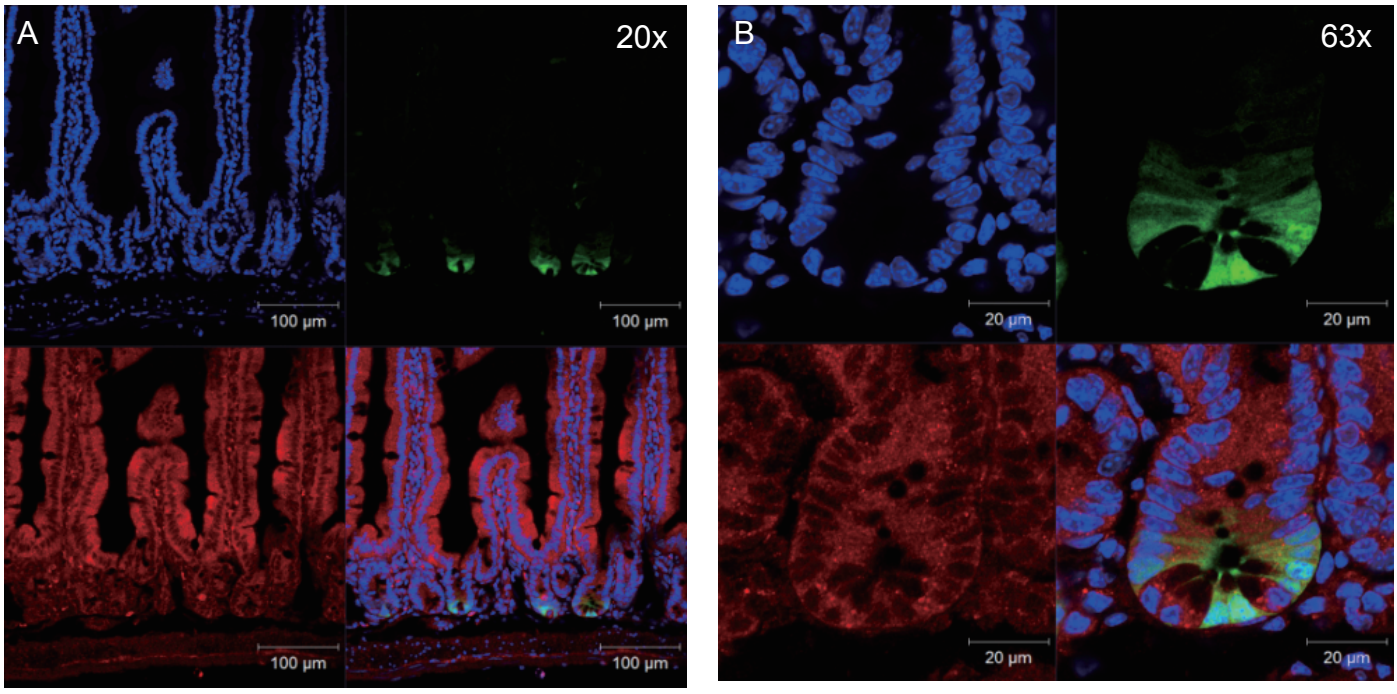

DAPI/Lgr5-eGFP/RhoA

C

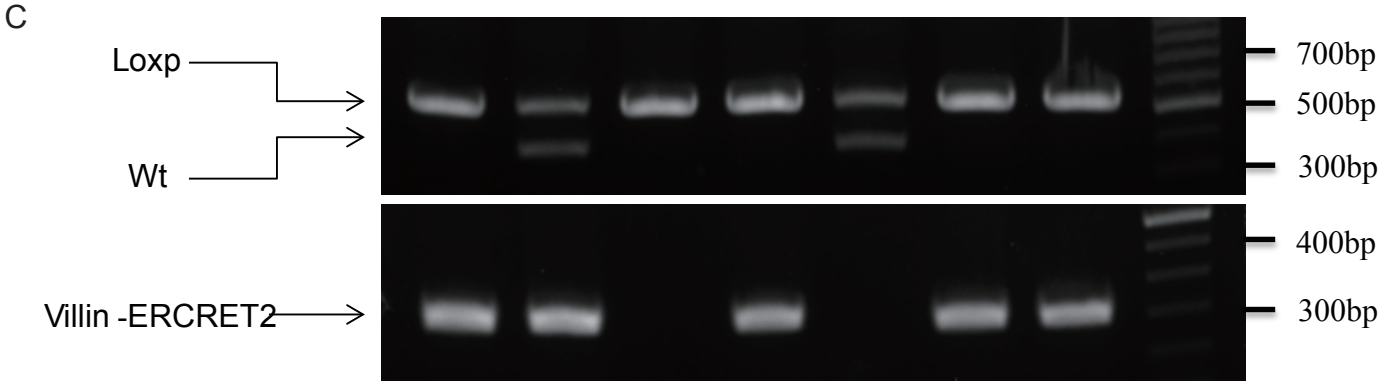

D

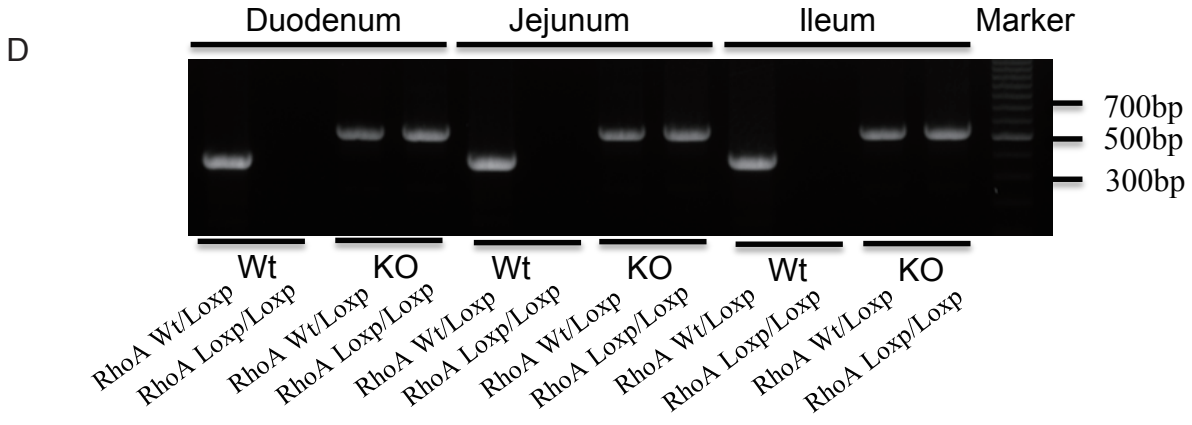

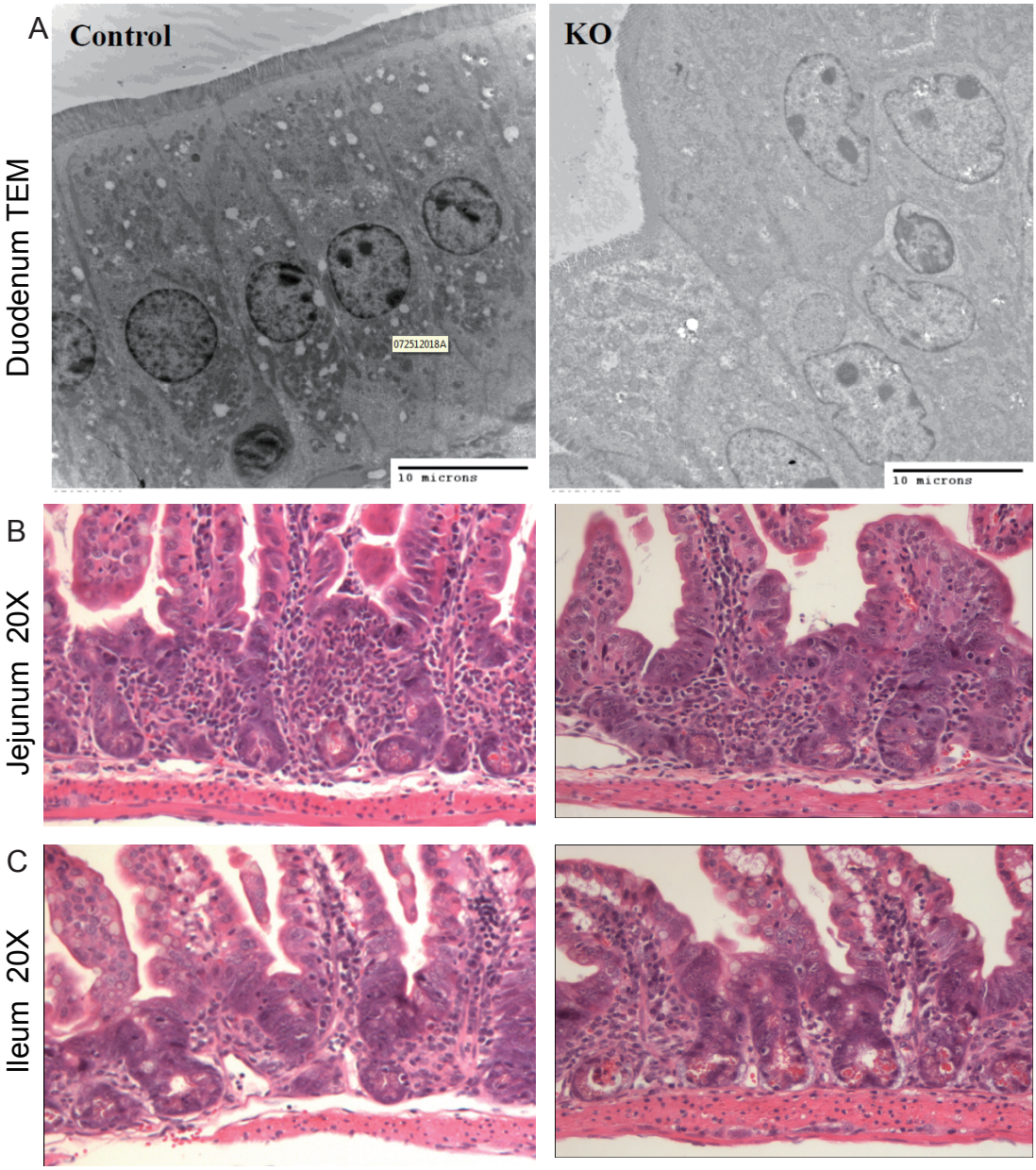
A
Control
KO
Duodenum TEM
072512018A
10 microns
10 microns
B
Jejunum 20X
C
Ileum 20X

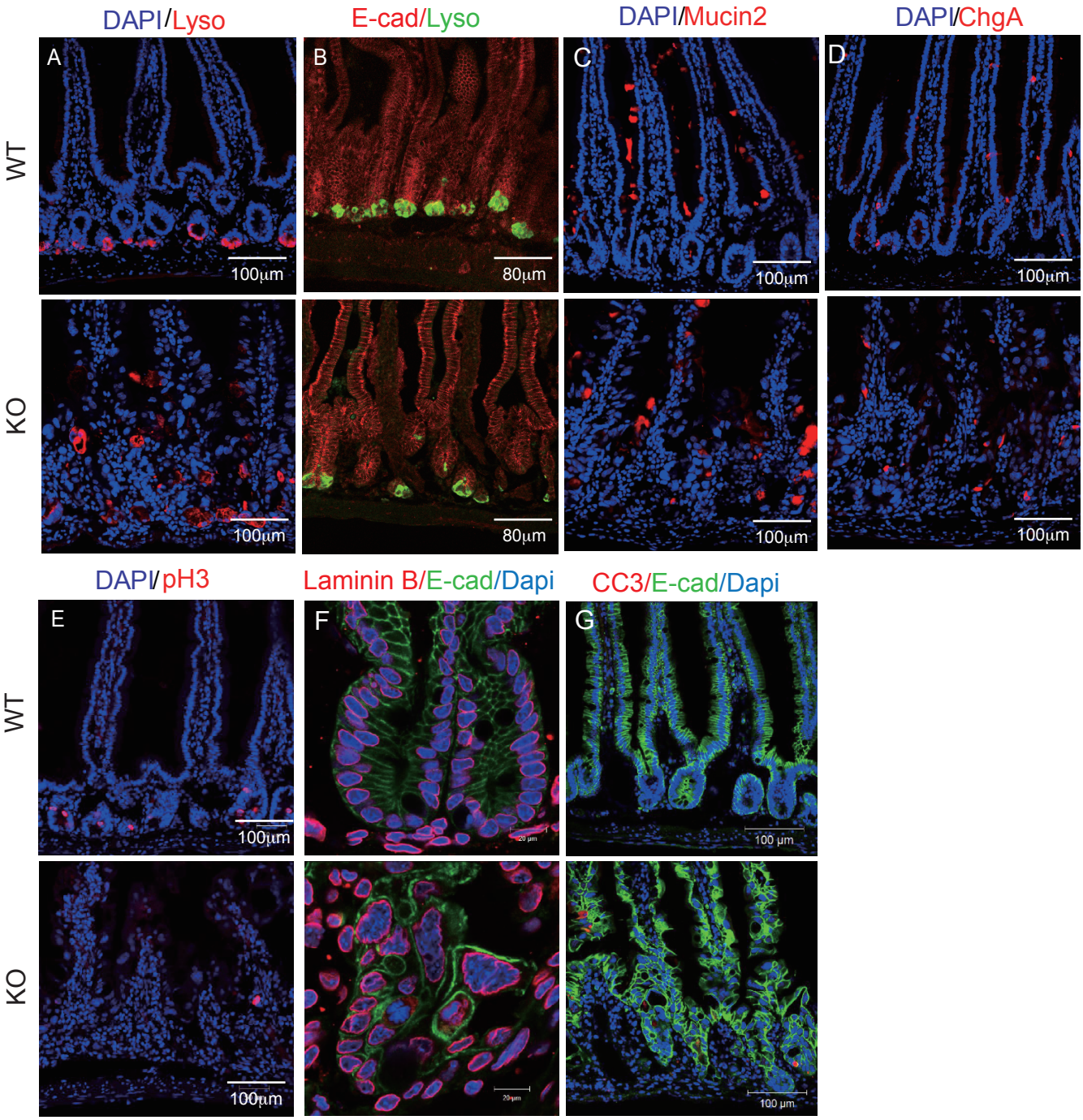
DAPI/Lyso
E-cad/Lyso
DAPI/Mucin2
DAPI/ChgA
A
B
C
D
WT
KO
100μm
80μm
100μm
100μm
100μm
80μm
100μm
100μm
DAPI/pH3
Laminin B/E-cad/Dapi
CC3/E-cad/Dapi
E
F
G
WT
KO
100μm
100μm
100 μm
100 μm

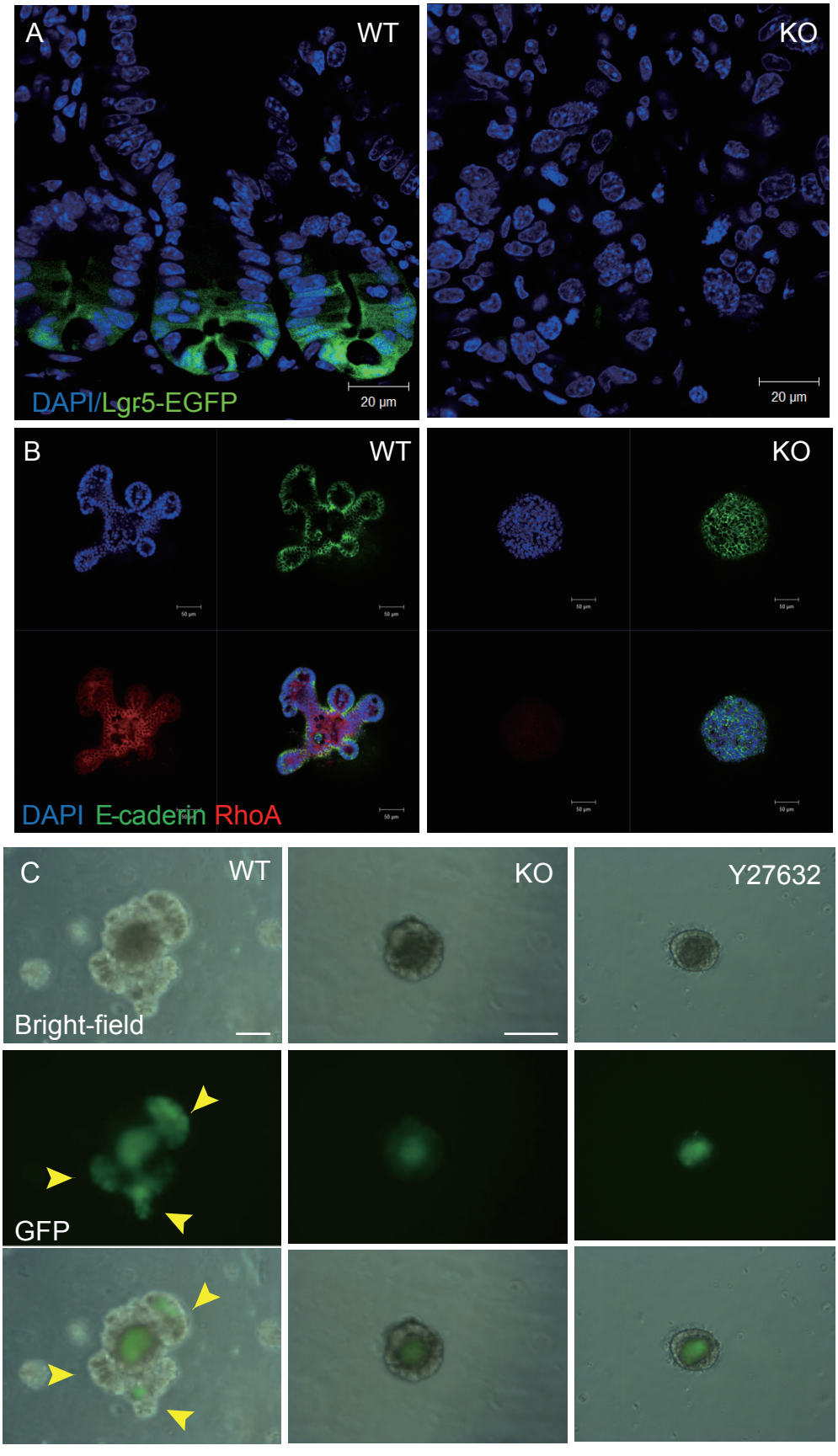
A
WT
KO
DAPI/Lgr5-EGFP
20 μm
20 μm
B
WT
KO
DAPI E-caderin RhoA
C
WT
KO
Y27632
Bright-field
GFP

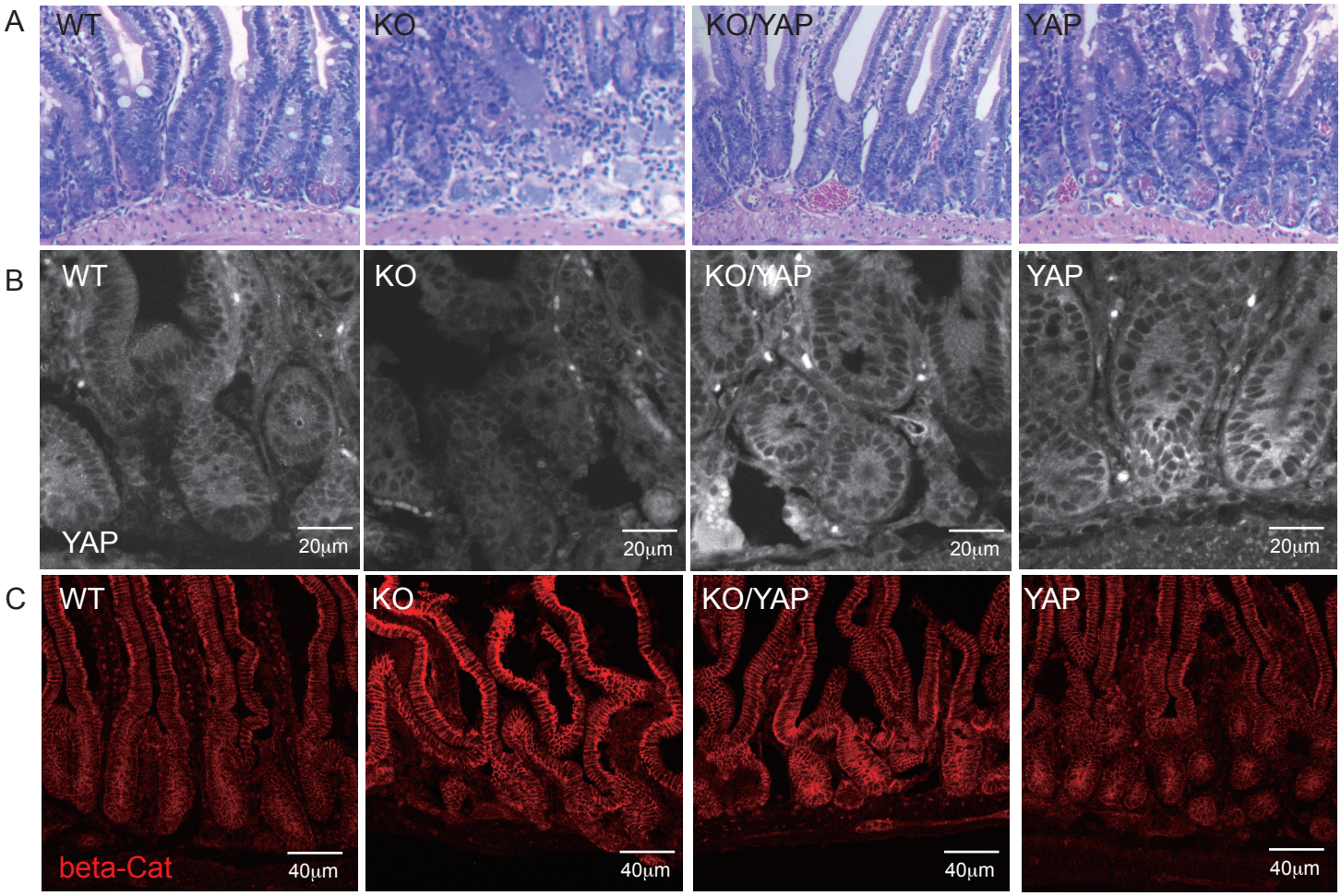
A
WT
KO
KO/YAP
YAP
B
WT
KO
KO/YAP
YAP
YAP
20μm
20μm
20μm
20μm
C
WT
KO
KO/YAP
YAP
beta-Cat
40μm
40μm
40μm
40μm

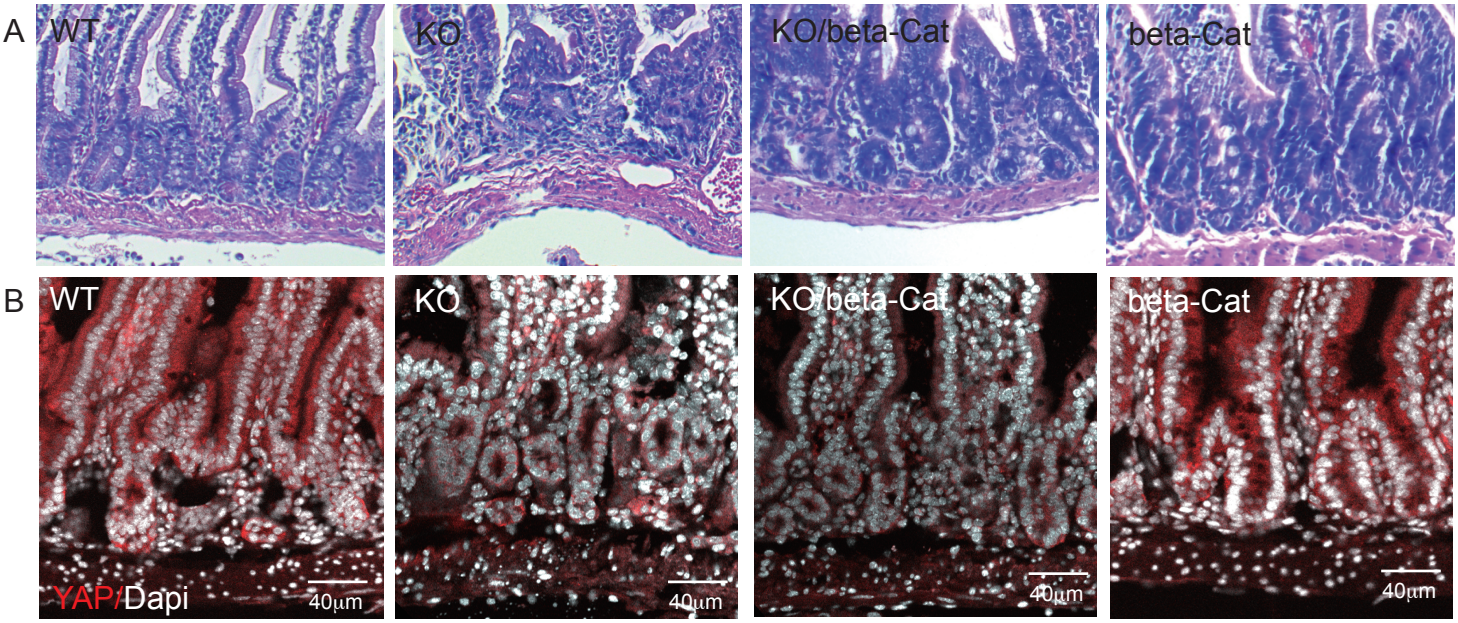
A
WT
KO
KO/beta-Cat
beta-Cat
B
WT
KO
KO/beta-Cat
beta-Cat
YAP/Dapi
40μm
40μm
40μm
40μm

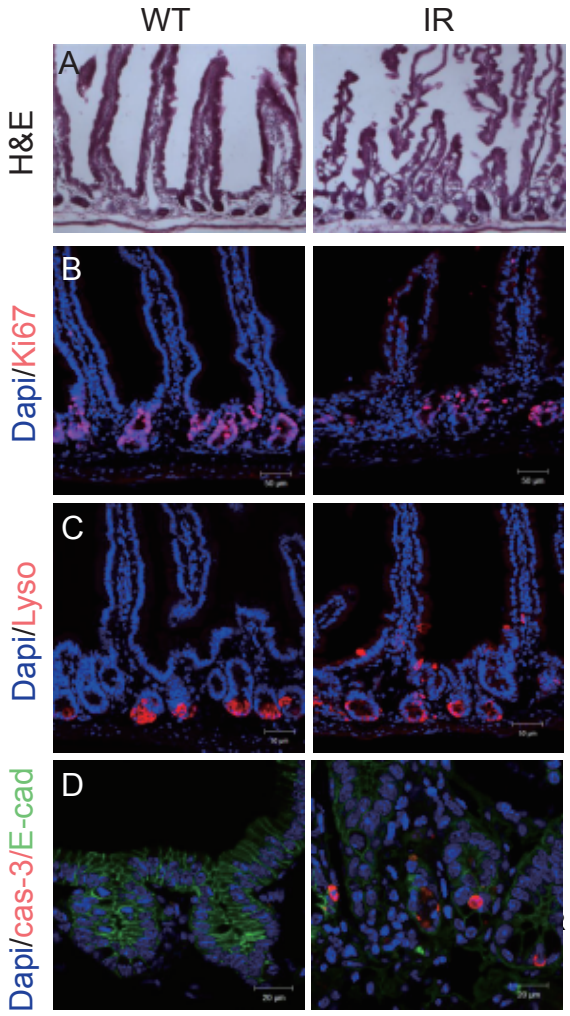
WT
IR
A
H&E
B
Dapi/Ki67
C
Dapi/Lyso
D
Dapi/cas-3/E-cad

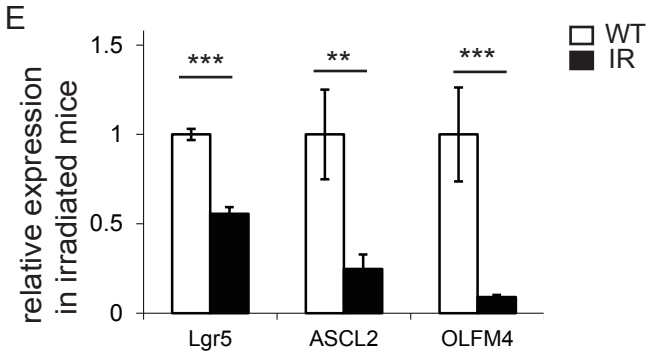
E
relative expression
in irradiated mice
1.5
1
0.5
0
***
**
***
WT
IR
Lgr5
ASCL2
OLFM4